KfK 5429
November 1994

European DEMO BOT Solid Breeder Blanket

Compiled by: Mario Dalle Donne
Contributors: Helmut Albrecht, Lorenzo V. Boccaccini, F. Dammel, U. Fischer, H. Gerhardt, K. Kleefeldt, W. Nägele, P. Norajitra, G. Reimann, H. Reiser, O. Romer, P. Ruatto, F. Scaffidi-Argentina, K. Schleisiek, H. Schnauder, G. Schumacher, H. Tsige-Tamirat, B. Tellini, P. Weimar, A. Weisenburger, H. Werle

Association KfK-Euratom
Projekt Kernfusion

Kernforschungszentrum Karlsruhe

KERNFORSCHUNGSZENTRUM KARLSRUHE

Association KfK - Euratom
Projekt Kernfusion

KfK 5429

European DEMO BOT Solid Breeder Blanket

Compiled by: M. Dalle Donne

Contributors: H. Albrecht, L.V. Boccaccini, F. Dammel, U. Fischer, H. Gerhardt, K. Kleefeldt, W. Nägele, P. Norajitra, G. Reimann, H. Reiser, O. Romer, P. Ruatto, F. Scaffidi-Argentina, K. Schleisiek, H. Schnauder, G. Schumacher, H. Tsige-Tamirat, B. Tellini, P. Weimar, A. Weisenburger, H. Werle

Kernforschungszentrum Karlsruhe GmbH, Karlsruhe

Kernforschungszentrum Karlsruhe GmbH
Postfach 3640, 76021 Karlsruhe

ISSN 0303-4003

European DEMO BOT Solid Breeder Blanket

Abstract

The BOT (Breeder Outside Tube) Solid Breeder Blanket for a fusion DEMO reactor is presented. This is one of the four blanket concepts under development in the frame of the European fusion technology program with the aim to select in 1995 the two most promising ones for further development.

In the paper the reference blanket design and external loops are described as well as the results of the theoretical and experimental work in the fields of neutronics, thermohydraulics, mechanical stresses, tritium control and extraction, development and irradiation of the ceramic breeder material, beryllium development, ferromagnetic forces caused by disruptions, safety and reliability. An outlook is given on the remaining open questions and on the required R&D program.

"This work has been performed in the framework of the Nuclear Fusion Project of the Kernforschungszentrum Karlsruhe and is supported by the European Communities within the European Fusion Technology Program."

Europäisches DEMO BOT Feststoff-Brutblanket

Zusammenfassung

Es wird ein heliumgekühltes Feststoffbrutblanket für einen Demo-Fusionsreaktor mit Brutstoff außerhalb von Kühlrohren (BOT) vorgestellt. Dies ist eines der vier Blanket-Konzepte, welche im Rahmen des europäischen Fusions Technology Programms entwickelt werden mit dem Ziel, in 1995 die zwei aussichtsreichsten Konzepte für die weitere Entwicklung auszuwählen.

Im Bericht werden der Referenzentwurf für das Blanket und die dazugehörigen externen Kreisläufe beschrieben, und die Ergebnisse der theoretischen und experimentellen Arbeiten auf den Gebieten Neutronik, Thermohydraulik, mechanische Spannungen, Tritium-Handhabung und -Extraktion, Entwicklung und Bestrahlung des keramischen Brutstoffes, Berylliumentwicklung, elektromagnetische Kräfte verursacht durch Plasmazusammenbrüche, Sicherheit und Zuverlässigkeit aufgezeigt. Es wird ein Ausblick auf die noch verbleibenden offenen Fragen und das erforderliche F&E-Programm gegeben.

"Die vorliegende Arbeit wurde im Rahmen des Projekts Kernfusion des Kernforschungszentrums Karlsruhe durchgeführt und ist ein von den Europäischen Gemeinschaften geförderter Beitrag im Rahmen des Fusionstechnologieprogramms."

Table of Contents

1. Introduction

In the framework of the European Community Fusion Technology Program four blanket concepts for a DEMO reactor are being investigated. DEMO is the next step after ITER. It should ensure tritium selfsufficiency and operate at coolant temperatures high enough to have a reasonable plant efficiency. These investigations, which include R. & D. work, aim at a well founded choice among various concepts in view of developing blanket modules to be tested in ITER only for the most promising blankets.

Two of the four blankets are based on the use of a liquid metal breeder, the other two on the use of a solid breeder. The latter have many features in common: both use high pressure helium as coolant and helium to purge the tritium from the breeder material, martensitic steel as structural material and beryllium as neutron multiplier. The configurations of the two blankets are, however, different: in the B.I.T. (Breeder Inside Tube) concept the breeder material is $LiAlO_2$ or Li_2ZrO_3 in the form of annular pellets contained in tubes surrounded by beryllium blocks, the coolant helium being outside the tubes [1, 2], whereas in the B.O.T. (Breeder Out of Tube) the breeder and multiplier material are Li_4SiO_4 and beryllium pebbles placed between plates containing channels where the coolant helium is flowing. The present report deals with the BOT solid breeder concept.

The proposed solid breeder blanket materials have a high melting point, are not very chemically active and, of course, do not present MHD problems. If kept at sufficiently high temperature they readily release the tritium produced, making possible the tritium in-situ removal by a helium purge flow. Tritium extraction from helium is of course much simpler than from water or a liquid metal.

Helium is better suited than water as the coolant of a lithium ceramic blanket. Water reacts with lithiated ceramics producing lithium hydroxide, which has a relatively high vapor pressure. This, besides affecting the integrity of the ceramic, could cause unduly high lithium transport due to the temperature gradients present in the blanket. Furthermore, water at temperatures higher than 600 °C reacts also with beryllium producing hydrogen. In case of porous beryllium the reaction is selfsustaining. Helium, on the contrary, is an inert gas and, as the experience with helium cooled fission reactors shows, can be kept extremely pure (total amount of impurities <1 ppm) even in large and complex circuits. Unlike water, helium can be kept at high temperatures without need to increase the pressure, thus the problem of keeping the minimum temperature in the breeder material above a certain level, to ensure low tritium inventories in the breeder, becomes

much easier, as thermal insulating gaps between breeder and coolant are not required. A further advantage of helium is that leakages to the plasma chamber have much less severe consequences than water leakages.

The present design has developed in various stages [3, 4, 5], which, essentially, were improvements in view to solve the problems posed by the behavior of beryllium under irradiation and to increase the availability of the system. The design is based on the following principles:

a) The use of lithium orthosilicate (Li_4SiO_4) as breeder to have fast tritium release (low tritium inventory), high lithium density and low lithium partial pressure at high temperatures (low lithium transport).

b) The use of small Li_4SiO_4 pebbles to avoid thermal stress problems in the breeder material and to provide a well defined path for the helium purge flow.

c) The use of pebble beds of relatively small dimensions, especially in the vertical direction, to avoid thermal ratcheting of the container walls or excessive breaking up of the pebbles.

d) The use of a helium purge flow at atmospheric pressure to reduce the amount and probability of tritium losses and to reduce the mass flow rate of the purge gas system.

e) The use of the Breeder Out-of-Tube solution to keep the thickness of the coolant channels within reasonable limits.

f) Cool the first wall with cold (inlet) helium; keep the minimum temperature of the breeder above 300 - 350 °C to reduce the tritium inventory; keep the beryllium temperature as low as possible (reduce beryllium swelling).

g) Use of radial toroidal modules, which allow a good filling with breeder and multiplier of the space available in the blanket region and subdivision of the modules in submodules. This reduces the thermal stresses, makes precise construction easier and gives the possibility of making significant tests starting from the smaller submodules.

h) Use of a redundant convective cooling system and of a double containment against tritium losses for safety improvement.

2. Blanket Design

2.1 DEMO Specification

The common basis for the blanket selection process is a DEMO-reactor specified by a Test Blanket Advisory Group (TAG). This specification is not the result of a detailed reactor study but a set of boundary conditions and minimum requirements for breeding blankets. Table 2.1 [6] shows the main parameters of DEMO, largely derived from NET (Next European Torus).

Table 2.1 Selected DEMO specifications

Major radius [m]	6.3
Minor radius [m]	1.82
Aspect ratio	3.45
Plasma current [MA]	20
Fusion power [MW]	2200
Average neutron wall loading [MW/m^2]	2.2
Surface heat flux [MW/m^2]	0.4 average 0.5 peak
Reference operating mode	continuous
Impurity control	double-null divertor
First wall protection	none
Number of TF coils	16
Toroidal magnetic field on axis [T]	6
Number of segments	32 inboard, 48 outboard
Blanket/shield thickness [m]	0,86 (inboard) 1.86 (outboard)

The minimum requirements specified for all blanket concepts are:

- tritium self-sufficiency (taking into account 10 horizontal ports of 3 m height and 1 m width)

- full power life-time 20000 h, resulting in 70 dpa maximum first wall damage.
- coolant conditions sufficient for electricity generation with a thermal efficiency $\eta \geq 30$ % where η is defined as the ratio between the electricity production from the blankets to the sum of neutron power and surface heat flux to the blankets.
- blanket resistance to a major plasma disruption (current decay from 20 MA to zero in 20 ms) such that segments may be non operational but still be removable by standard exchange procedures.
- thermal and mechanical loads acceptable for the martensitic steel MANET.

2.2 Design Description

Fig. 2.1 shows a vertical cross section of the Demo blanket surrounding the plasma. Various horizontal sections are shown as well. The poloidal magnetic field has two points where it equals zero, and thus it is called a double-null configuration. The blanket is divided into two parts: an outboard and an inboard blanket.

The DEMO torus has 16 toroidal field (TF) coils. On the outboard side there are three blanket segments for each TF coil, two of them adjacent to the magnets and one in the middle. On the inboard side there are two segments. Altogether there are 48 outboard segments with an opening angle of 7.5 ° in respect of the torus axis of symmetry and 32 inboard segments with an opening angle of 11.25 °. These arrangements facilitate the loading and unloading of the blanket segments. In order to increase the breeding capability, the blanket of the inboard segment is extended to the area behind the divertors and the blanket of the outboard segment is prolonged by a vertical part arranged at the upper segment section on the opposite location to the upper divertor. This is in accordance with the specifications of the European Test Blanket Advisory Group.

The radial shielding forms part of the blanket segments. The radial thickness at the midplane of the inboard segment amounts to 856 mm and of the outboard segment to 1856 mm. The total length of the blanket segments amounts to approx. 16 m. The blanket segments except the lower part of the inboard segment are suspended from the flange of the upper access port. This port serves for the exchange of blanket segments. The following considerations concern a lateral inboard and a central outboard blanket segment.

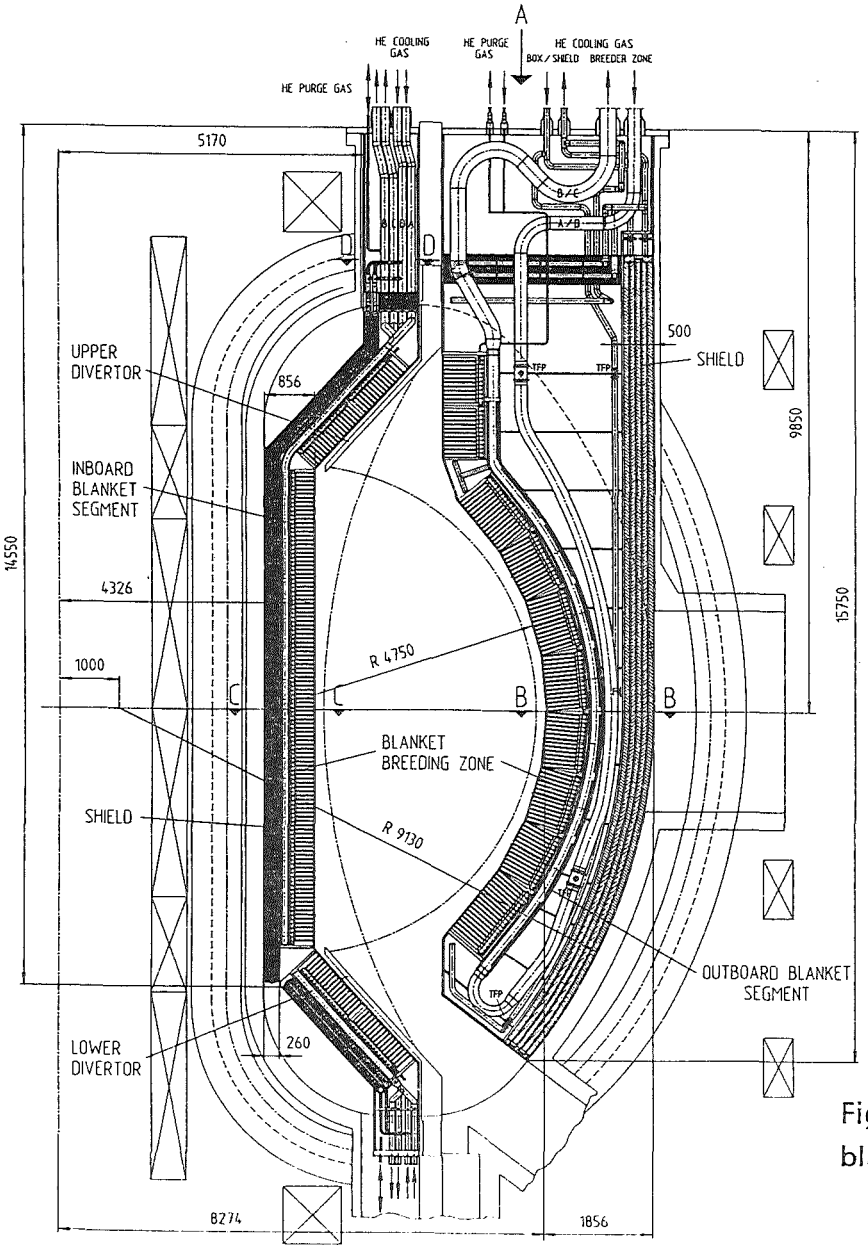

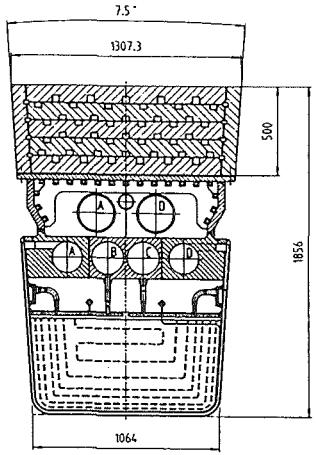

SECTION B-B

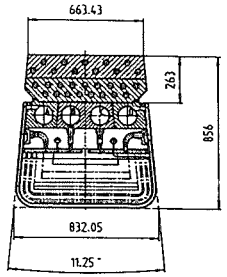

SECTION C-C

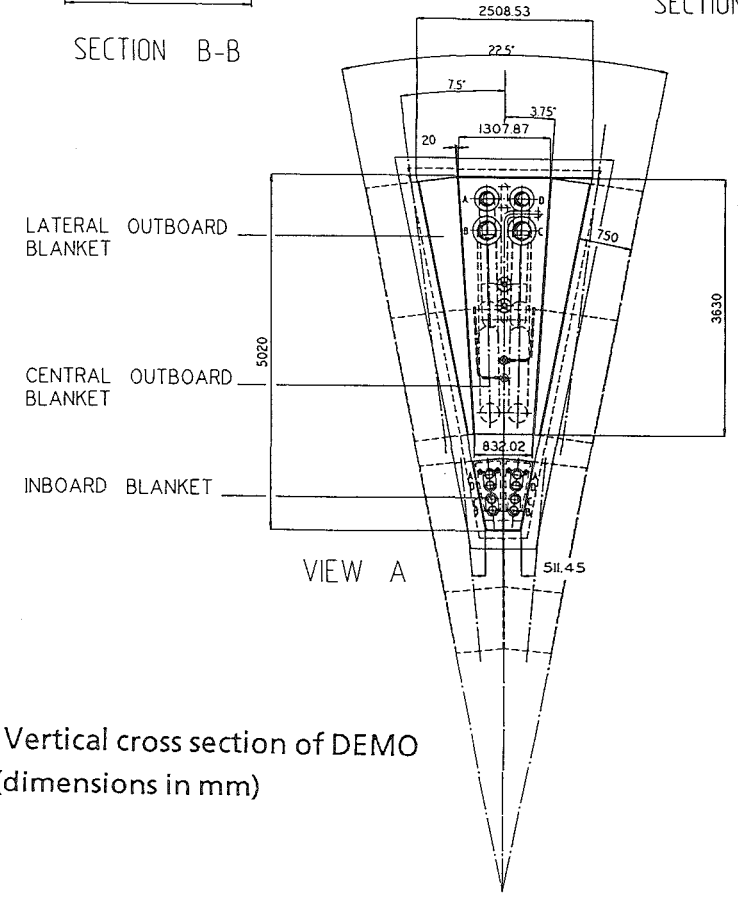

VIEW A

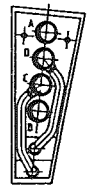

SECTION D-D

Fig. 2.1: Vertical cross section of DEMO blanket (dimensions in mm)

2.2.1 The outboard blanket segment

The outer blanket segment is illustrated in Figs. 2.1 through 2.4 and exhibits the following basic design features:

1. The ceramic breeder material (Li_4SiO_4 pebbles) and the neutron multiplier (beryllium pebbles) are contained in 10 poloidal sections (Fig. 2.1)
2. The whole arrangement of these sections is contained in a tightly closed box called a blanket box (Fig. 2.2).
3. The plasma facing surface of the blanket box is called the first wall (F.W.). The back side of the blanket box is formed by a plate which contains the poloidal coolant helium feeding manifolds (Fig. 2.2).
4. At the back of the blanket box there are the main coolant helium feeding tubes. These are contained in a closed box which is welded to the back of the blanket box. Blanket box plus feeding tubes box form the segment box (Fig. 2.1, section B-B).
5. A helium cooled vertical radial shield is provided at the back of the segment box (Fig. 2.1).
6. A horizontal shield is installed inside the segment box upper part above the blanket (Fig. 2.1).
7. The blanket box and blanket structure are cooled by helium at 8 MPa. The coolant flows in series through the blanket box and the blanket structure.
8. The blanket structure consists of 8 mm thick cooling plates placed in toroidal-radial planes. The plates are welded to the front and side walls of the blanket box (Fig. 2.2 and 2.3).
9. Alternatively between the plates there are slits of 11 mm thickness filled by a bed of 0.3 to 0.6 mm diameter Li_4SiO_4 pebbles, or of 45 mm thickness filled by a binary bed of 1.5 to 2.3 mm and 0.08 to 0.18 mm beryllium pebbles (Fig. 2.3).
10. A separate purge gas system at 0.1 MPa carries away the tritium generated in breeding material and in beryllium.
11. For safety reasons, the coolant flow is divided into two completely independent coolant systems, which feed in series the FW cooling channels and then the coolant plates in alternating directions.

The general arrangement of the cooling systems is shown in Fig. 2.1. The blanket box is formed by first wall / radial walls containing radial / toroidal / radial cool-

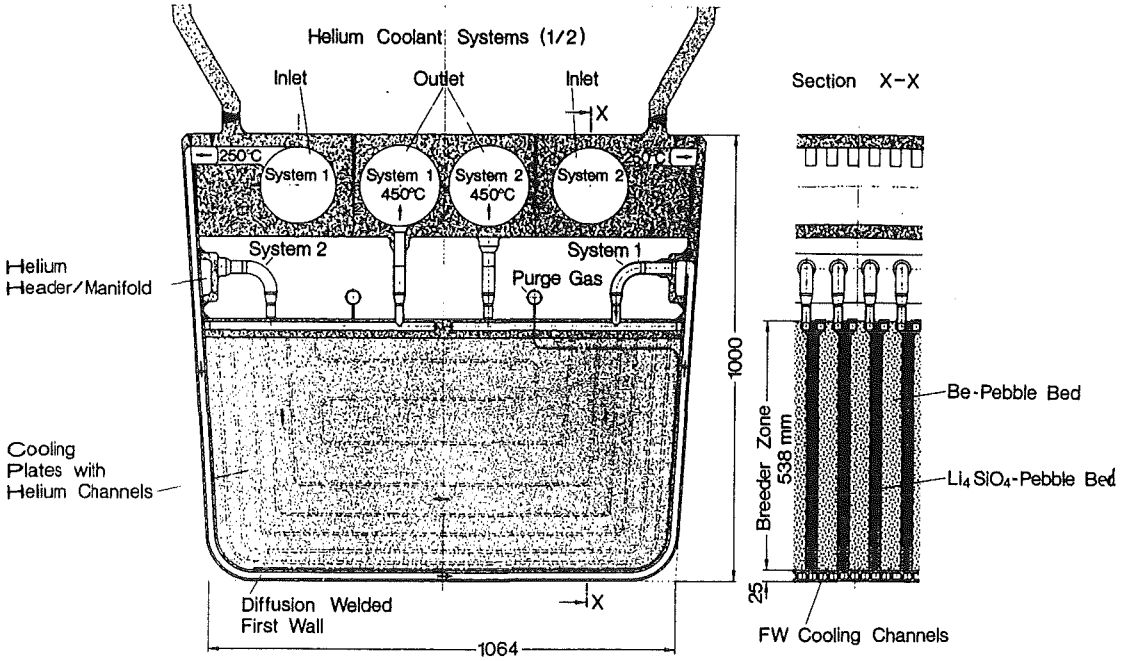

Fig. 2.2: Horizontal cross section of the outboard blanket segment at the equatorial plane of the torus (left) and vertical cross section of the same (right).

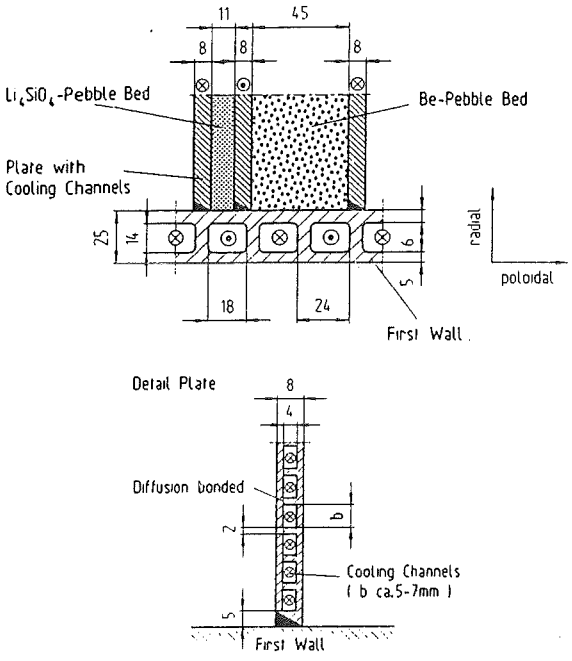

Fig. 2.3: Poloidal-radial cross section: detail showing the arrangement of the helium cooling channels in the first wall and in the cooling plates.

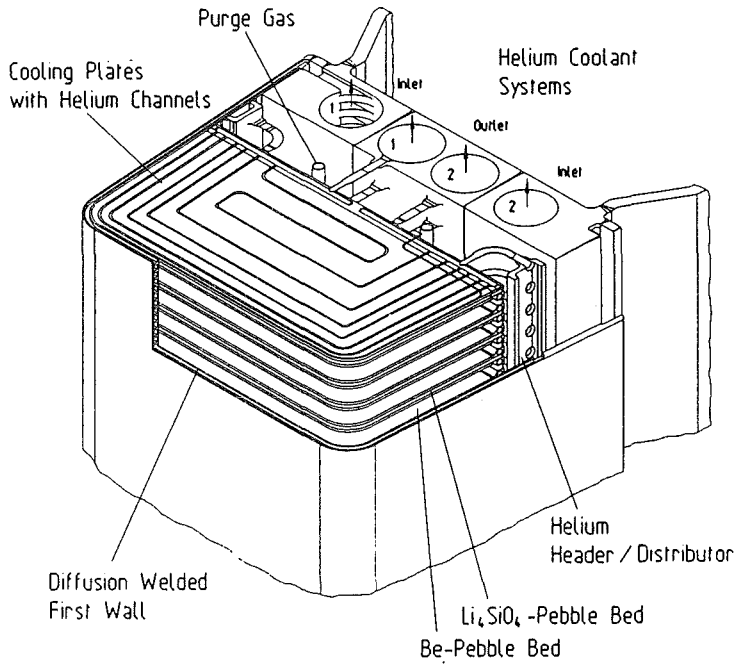

Fig. 2.4: Isometric view of a poloidal portion of the outboard blanket segment around the torus equatorial plane.

ing channels and the back wall with integrated poloidally running cooling gas manifolds. It is a closed box with helium-cooled cover plates at top and bottom. The main coolant feeding tubes (A/D) are connected to the manifolds at the bottom, the main outlet tubes (B/C) at the top of the blanket. The purge gas inlet and outlet lines are connected to the respective manifolds at the top of the blanket box. The cooling and the purge gas main tubes inside the segment box are routed in such a way (e.g. with expansion bends) that stresses due to different thermal expansion are well below allowable limits.

The cooling gas feed tubes are fixed to the segment side walls by semi-fixed points (clamps) to withstand forces from plasma disruptions and to keep the stresses in the pipe walls within acceptable limits (see Fig. 2.1). To reduce the induced electrical currents in the structures caused by plasma disruptions, the clamps are electrically insulated from the pipes. The piping outside the blanket box is surrounded by the segment box, of which the first wall and the side walls of the blanket box are an integral part.

The segment box side walls are helium-cooled by brazed poloidal cooling tubes. The cooling gas inlet is at the bottom also providing coolant to the bottom plate. The outlet collectors are arranged at the segment top below the horizontal shield. The segment box is stiffened by horizontal U-shaped stiffening plates to provide stronger resistance against forces from plasma disruptions. The pipe fixing clamps are connected to the stiffening plates (Fig. 2.1).

A horizontal shield is installed inside the segment upper part above the blanket to protect flange region and piping arrangement located there from neutron irradiation and to limit the radiation level at the space above the flange. This shield consists of a helium-cooled welded structure filled with granulated shielding material. Cooling is provided by embedded cooling tubes (Fig. 2.1).

The pipings for blanket cooling gas, purge gas and coolant for the segment walls penetrate the horizontal shield, and are routed with expansion bends to the segment flange. The penetration through the flange plate has to be a gas-tight welded structure, also providing the fixing points for the supply lines (Fig. 2.1).

A radial shield is provided at the back of the segment box. The function of this shield is to protect the vacuum vessel and the magnetic field coils from excessive radiation. The radial shield is mechanically attached to, but, if needed, electrically insulated from the back wall of the segment at the outside. It is a welded steel structure of 500 mm total thickness provided with poloidally running cooling channels and helium cooling. The cooling gas inlet and outlet pipes are arranged at the top of the shield and are connected in parallel to the cooling system of the

segment walls inside the segment box (Fig. 2.1). The coolant flow in the shield structure is directed downwards in the front part and upwards in the rear part. The radial shield of the outboard segment is designed in such a way that it can be disconnected from the segment box and be possibly re-used without cutting and re-welding.

The blanket box cooling channels depart from the poloidal manifold feeding channels and run first toroidally, then radially, then again toroidally to cool the first wall, and finally radially to poloidal short manifolds welded to the side wall of the box. The helium flows in opposite directions in the two cooling systems. This allows a more uniform temperature field in the first wall and in the blanket and avoids the nonsymmetrical thermal expansion in poloidal direction of the blanket box due to the helium temperature increase in the first-wall region (Fig. 2.2).

There are two poloidal short manifolds per blanket poloidal section. The helium is carried to the coolant plate by a 90° bended tube, then it goes into a toroidal distribution tube welded in the plate (Fig. 2.2) and finally in many parallel radially-toroidally running channels contained in the plate, which cool the ceramic material and the beryllium multiplier. These coolant channels are shown only schematically in Fig. 2.2. For a more detailed description of the cooling channels see Section 2.5. After leaving the cooling plate the helium is collected by means of radial tubes to the poloidal manifolds contained in the back plate of the blanket box (Fig. 2.2) and finally flows through the two outlet tubes (Fig. 2.1).

Fig. 2.3 shows the arrangement of the helium cooling channels in the first wall and in the cooling plates. The upper part of the picture shows how the blanket cooling plates are welded to the first wall, while the lower shows a detail of the cooling channels of the cooling plates. Due to the higher thermal conductivity of the Be pebble bed, its thickness is greater than that of the Li_4SiO_4 bed. Both the first wall and the blanket cooling plates are manufactured by diffusion welding. At both ends of the blanket poloidal section the blanket box is connected to the next section by means of two independent electron beam welds with a monitoring gap in between to improve the availability of the system (see Section 2.3). The size and arrangement of the feeding tubes and manifolds for the leak detection system (not shown in Fig. 2.1) are similar to those of the purge gas.

Fig. 2.4 shows an isometric view of a poloidal portion of the outboard blanket segment. One can clearly see the two independent cooling systems containing high pressure helium. The helium purge gas is distributed inside the blanket box by small poloidal manifolds. Small tubes placed in toroidal radial planes bring the

purge flow to the front of the blanket, near the first wall, in each pebble bed (beryllium or Li_4SiO_4) slit. Then the gas exits the tube by small perforations and moves in radial direction towards the back of the blanket. There it is collected in a second small poloidal manifold (Fig. 2.2 and 2.4) and brought toward the top of the blanket box.

2.2.2 The inboard blanket segment

The inboard blanket segment mainly consists of blanket box, piping and radial shield, all contained in the segment box. A horizontal shield is installed in the upper segment region to protect from neutron irradiation the TF-coils, the flange region and the piping above (Fig. 2.1).

The inboard blanket segment is divided into a main part and a small part arranged behind the lower divertor. The lower small blanket has the same layout as the upper main part but is supplied with cooling and purge gas through the bottom of the vacuum vessel. However, it has to be exchanged also through the upper access port (Fig. 2.1).

The inboard blanket segment has the same general arrangement of blanket box and shield as the outboard blanket segment. However, the radial shield of the inboard segment is integrated into the segment box. The back plate of the blanket box contains the poloidally running manifolds for the twofold redundant coolant system (Fig. 2.1, section C-C).

Coolant and purge gas supply lines are connected at the top to the respective manifolds. The supply lines penetrate the horizontal shield above the blanket and exit the segment through bellows welded to the segment flange to allow thermal expansion of the pipings (Fig. 2.1). Due to the small place available at the neck in the upper region of the inboard boxes (see view A in Fig. 2.1), the diameter of the coolant helium feeding tubes is relatively small (132 mm o.d.). However, at variance to the previous case with helium cooling tubes [4], the considerably lower helium cooling pressure drop due to the use of many parallel channels in the coolant plates, allows to maintain also with the inboard blanket the helium pressure at the level of 8 MPa.

The radial shield consists of steel blocks with cooling channels which are welded together. The steel blocks should contain 10 ÷ 20 % zirconium hydride pellets to reduce the neutron fluence in the vacuum vessel and in the magnets below allovable limits (see Section 2.4). The radial shield is cooled by a bypass flow of he-

lum which is separated from the main coolant flow above the horizontal shield.The downward flow is at the front part of the shield, turned at the bottom into opposite direction and the upward flow is at the rear side. The lower shield structure is extended below the blanket box to provide enough shielding at that area (Fig.2.1).

2.3 Fabrication and Assembly

The fabrication and assembly of the blanket segments is performed in the following steps:

1. Fabrication of the first wall (FW) sections with a poloidal length of approximately 1 meter: first the grooves forming the FW cooling channels are milled and the two plates are bounded together by diffusion bonding (also called diffusion welding). Afterwards the plates are bended to form the FW and the side walls of the blanket box (Fig. 2.1 and 2.2).
2. Fabrication of the blanket cooling plates: also these plates are fabricated by milling the cooling channels and bonding them by diffusion bonding. Afterwards the toroidal manifolds are welded to the plates (Fig. 2.2).
3. Welding of the blanket cooling plates to the FW and side walls of the box section (Fig. 2.4): filling of the slits between the plates with the Li_4SiO_4 and beryllium pebbles. Closing the slits at the back side with porous plates to allow the passage of the helium purge flow (Fig. 2.2).
4. Welding of the short poloidal manifolds to the side walls of the box section. Welding of the bended tubes between these manifolds and the plates (Fig. 2.2).
5. EB welding of the various poloidal sections (Fig. 2.1).
6. Welding of the straight tubes from the cooling plates to the central part of the back plate containing the two outlet helium manifolds (Fig. 2.2).
7. Welding of side parts of the back plate to side walls of the box and to the plate central part. Finally, welding of two longitudinal plates to the side plates to close the box (Fig. 2.2).
8. After having closed the blanket box by welding the end plates at the top and bottom, the connections to the feeding tubes can be made and the back side of the segment box can be welded to the blanket box (Fig. 2.1).
9. Afterwards, the shield can be bolted to the back of the segment box and connected by means of flanges to its helium feed tubes.
10. At the end the segment box is proofed with leak and pressured tests.

All the welds connecting the blanket box to the exterior are double welds with an intermediate gap connected to the leak detection system. This of course improves the availability of the blanket. The availability is also improved by the fact that no high leak tightness is required between the parallel coolant channels of the blanket cooling plates. Furthermore, operation with small leakages at the plate boundaries is allowed, as the box can operate at the full helium coolant pressure (see Section 2.5).

The important aspects of this fabrication method are:

1. the diffusion bonding of the FW and of the cooling plates;
2. the U-bending of the blanket box walls;
3. the welding of the poloidal sections of the box walls and of the blanket coolant plates to these walls.

Work is being performed and/or will be performed in collaboration with industry and other organizations on these three points.

Diffusion bonding tests were performed on behalf of KfK by the Forschungsinstitut für Kerntechnik und Energiewandlung, Stuttgart, with a view to developing a technique by which MANET plate components equipped with coolant channels are manufactured by diffusion bonding. By this bonding technique two plates are pressed together in vacuo for a specified duration at mechanical pressure and temperatures up to approx. 1000 °C. On the faces to be joined material diffusion occurs which produces firm bonding of the parts.

In a first test series involving small specimens, 80 mm in diameter, provided with coolant and inspection channels the most favorable bonding parameters were determined for conditioning of the surfaces of the faces to be joined and for pressure and temperature. After heat treatment of the bonded specimens a leak test was carried out at 10 bar internal pressure and, in addition, metallographic investigations and bending tests were performed with specimens made of bonded material and - for comparison - with those made of the base material. All specimens were found to be tight. The best bonding results have been obtained for specimens with finely ground surfaces - roughness $\leq$ 3 µm - and bonding temperatures of 980 °C and 1050 °C. The pressure applied during bonding was 30 MPa and 18 MPa, respectively, for one hour and thereafter 7 MPa. Bending tests with these specimens showed that the strength was nearly the same to that of the base material.

In a next step three specimen plates, 320 mm in diameter, with a coolant channel geometry typical of the first wall, were bonded. Subsequent leak tests at 80 bar and 150 bar internal pressure provided evidence of tightness conforming to the detection limit of the instrument used in the leak tests.

U-bending of the box walls appears in principle feasible as the diffusion weld will be positioned in the neutral plane of the double plate and the bending radii are not too small (86° and 96° for the outboard and the inboard segments respectively). However, bending tests for representative diffusion bonded plates of MANET will be carried out in 1995.

The EB welding of the poloidal sections of the box walls has been already studied by industry on behalf of KfK [7, 8] for the FW of the Dual Coolant Blanket Concept [9]. This wall is quite similar to the present one and fabricated in the same way, thus the positive results for this FW can be applied to the welding of the poloidal sections for the present design. The welding of the blanket cooling plates to the box walls, however, is quite different. Thus a similar study is required. This will be performed during 1995.

2.4 Neutronics Analysis

The neutronics analysis is based on three-dimensional Monte Carlo calculations with the MCNP-code [10] and nuclear cross-section data from the European Fusion File EFF [11]. A geometrical model has been set up for a 11.25° torus sector of the DEMO-reactor (1/32 of the torus) with one inboard and one and a half outboard segments. Reflecting boundary conditions are applied at the lateral walls of the modelled torus sector. The model includes the vacuum chamber, first wall and blanket segments, the vacuum vessel, top and bottom divertor as well as a bottom divertor exhaust chamber with a pumping duct entrance. A heterogeneous array of helium cooling plates, beryllium and ceramics pebble beds has been integrated in the blanket boxes according to their technical layout. Fig. 2.4-1 shows a radial-poloidal cross-section of the MCNP torus sector model.

The spatial neutron source distribution is sampled in a special FORTRAN routine linked to the MCNP-code, for details see U. Fischer [12]. The following plasma parameters are used for the DEMO-reactor [3]: Major plasma radius = 630 cm, minor plasma radius = 182 cm, elongation = 2.17, excentricity = 16.2 cm, maximum triangularity = 0.57.

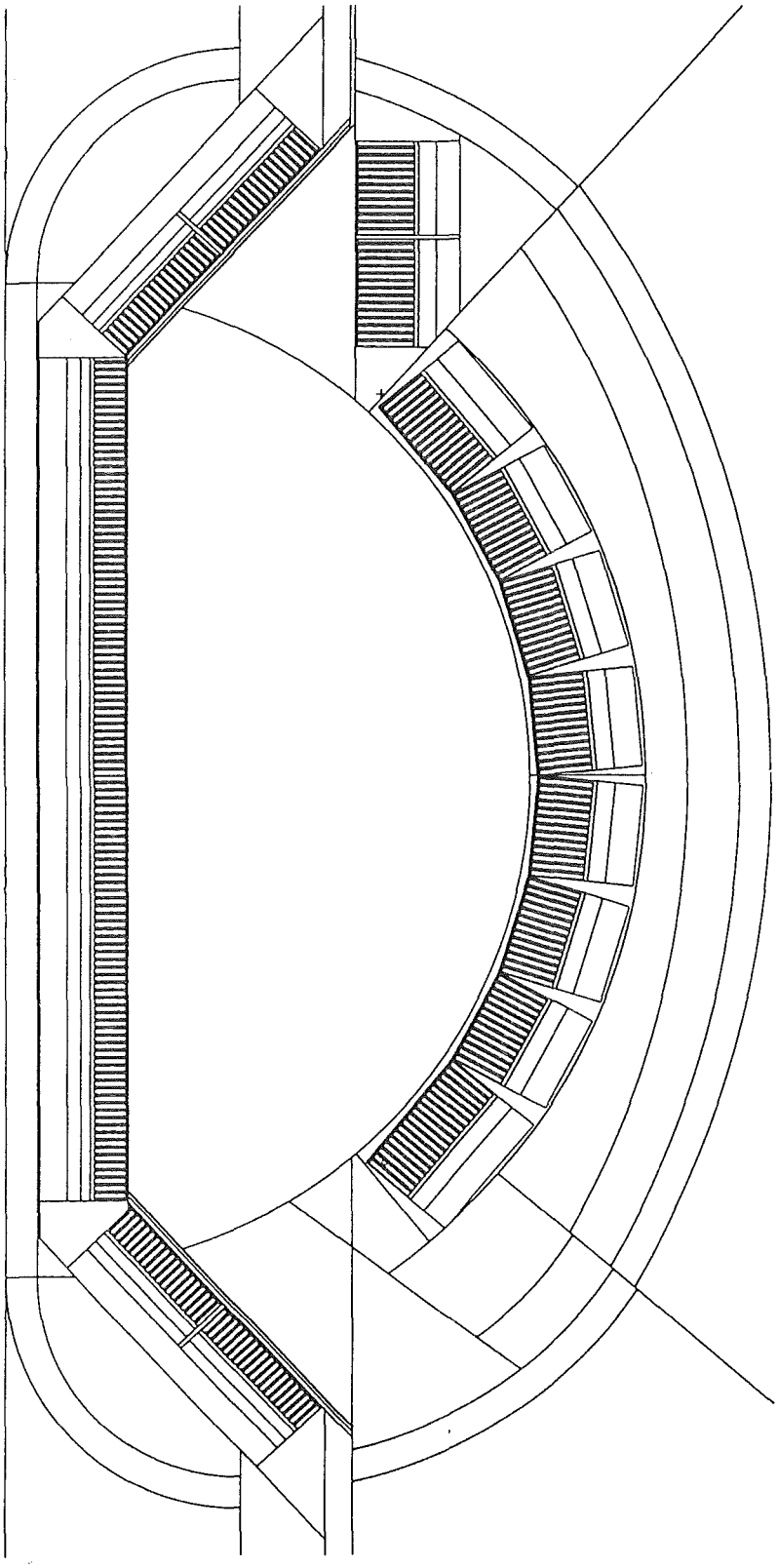

Fig. 2.4.1: Radial-poloidal section of the 11.25° torus sector model.

2.4.1 Tritium breeding ratio

The use of a beryllium neutron multiplier ensures a high tritium breeding potential for solid breeder blankets. Ideally it should be arranged with the breeding material in a homogeneous mixture at high volume fractions [13]. The drawbacks that arise by using a heterogeneous array of alternating beryllium and ceramics ceramic pebble bed layers separated by helium cooling plates, however, can be coped with, even at low ^{6}Li-enrichments.

In the present design a ^{6}Li-enrichment of 25 at% is assumed for the breeding material Li_4SiO_4 being contained as a pebble bed in radially-toroidally arranged channels of 11mm thickness at a packing factor of 64 %. The beryllium pebble bed, being composed of double size beryllium pebbles, is contained in 45 mm thick channels at a packing factor of about 80 %. The total radial thickness of the breeder zone amounts to 30 cm and 54 cm, inboard and outboard, respectively. In addition, the divertor region is utilised for breeding.

For calculating the global three-dimensional tritium breeding ratio (TBR) 120,000 source neutron histories have been followed in the Monte Carlo calculation. Table 2.4-1 shows the neutron balance and the associated statistical errors obtained in the TBR-calculation. The large beryllium mass inventory of the blanket (about 300 tons in total) results in a high neutron multiplication factor which is necessary to allow the low ^{6}Li-enrichment. Note that the beryllium mass inventory can be reduced without losses in the TBR by using a Li_4SiO_4 pebble bed without beryllium in the divertor breeding region and the upper blanket segment boxes at the outboard side [3].

Table 2.4-1 Neutron balance

Neutron multiplication	1.75 ± 0.1%
Tritium breeding ratio	
Outboard blanket segment	0.79 ± 0.4%
Inboard blanket segment	0.25 ± 0.7%
Divertor breeding region	0.09 ± 1.1%
Total tritium breeding ratio	1.13 ± 0.3%

Tritium breeding will be affected by the presence of blanket ports for plasma heating, remote handling, pellet injection, diagnostics etc.. Ten horizontal ports

centred at the equatorial plane of the outboard blanket segments are foreseen for the DEMO-reactor. Each blanket port covers an area of 340 cm height times the full segment width. The impact on the breeding performance of both liquid metal and solid breeder blankets has been assessed previously [14]. Based on these results, the global TBR is expected to decrease to about TBR = 1.07 in the presence of ten ports.

2.4.2 Power generation

For calculating the nuclear power generation a coupled neutron-photon Monte Carlo transport calculation has been performed. About 370,000 source neutron histories were followed in this calculation. The normalisation was performed for a fusion power of 2200 MW. Table 2.4-2 shows the resulting power generated in the inboard and outboard blanket segment. In the 32 inboard and 48 outboard blanket segments of the DEMO-reactor a total power of 2043 MW would be produced. This does not include the power generated in the shields and the divertor plates and the power radiated from the plasma.

Table 2.4-2 Nuclear power generation [MW] in the blanket segments (2200 MW fusion power)

Outboard blanket segment (7.5°)	30.7
Inboard blanket segment (11.25°)	
Central part	14.3
Divertor breeding region	3.5
Total inboard	17.8

A fine radial segmentation scheme has been introduced in the Monte Carlo calculation to obtain the radial power density distribution in the blanket boxes. The radial power density profile is comparatively flat in the ceramics due to the low ^{6}Li-enrichment. The Li_4SiO_4 peak power density is 37.0 W/cm^3 in the central outboard blanket box. It decreases to 28 W/cm^3 across the first 20 cm, and, further, to 11 W/cm^3 across the next ones. At the end of the breeding zone it is 6.5 W/cm^3. For the first wall the peak power density is 25.4 W/cm^3, and for the helium cooling plates it is 21.8 W/cm^3. For beryllium the peak power density is 14.9 W/cm^3 in the central outboard blanket box.

2.4.3 Afterheat generation

A detailed analysis of the afterheat generation has been performed [15] by combining three-dimensional Monte Carlo transport calculations with the MCNP-code and afterheat calculations with the FISPACT [16] inventory code. Neutron spectra were calculated in 175 energy groups (VITAMIN-J structure) in the first wall, the breeding zone and the blanket back shield for the blanket segment boxes at the outboard and inboard side and the divertor region. About 600,000 source neutron histories were followed in the MCNP-calculation for the spectra to assure a sufficient statistical accuracy. FISPACT inventory calculations were performed for the first wall, the breeding zone and the blanket back shield of the mentioned reactor components. The cross-section data of the European Activation File EAF-3 [17] were used in the FISPACT-calculations.

Table 2.4-3 shows the total afterheat power calculated for the central outboard blanket segment at reactor shut down (t = 0). An integral operation time of 20,000 hours at a fusion power 2200 MW is assumed in this calculation. The decay heat typically amounts to 2 % of the direct power generation. The rather large afterheat generation in the divertor region is caused by the inclusion of the divertor plates in the calculation. According to the specifications of the test blanket advisory group it consists of a 5 mm thick tungsten and a 30 mm thick copper layer supported by a 40 mm thick steel plate. Both tungsten and copper give rise to a large afterheat generation which amounts to 7 % of the direct heating power in the divertor region.

When excluding the divertor plates, MANET, the breeding ceramics and beryllium typically contribute to the afterheat power by 65, 5 and 30 %, respectively. The corresponding contributions to the direct power generation amount to 15, 45 and 40 %, respectively. The afterheat generation in beryllium is decreasing very fast (within a few seconds) to a low level because it mainly originates from the short-lived isotope $^{6}He(T_{1/2} = 0.8$ s). There is a large contribution to the afterheat of the breeding ceramics of the short-lived activation product $^{28}Al(T_{1/2} = 2.25$ m) immediately after shutdown; afterwards the afterheat of the breeding ceramics is dominated by tritium. The decay heat generation for MANET is roughly constant over the time period of a few minutes after shutdown. According to the half life of the main contributor ^{56}Mn ($T_{1/2} = 2.58$ h) it further decreases by one order of magnitude after one day.

Table 2.4-3 Afterheat generation [MW] in the blanket segments at reactor shutdown (2200 MW fusion power, 20000h irradiation)

	Direct heating power	Decay heat power
Outboard blanket segment (7.5°)		
Central part	28.9	0.588
Upper boxes	1.83	0.032
Total outboard	30.7	0.620
Inboard blanket segment (11.25°)		
Central part	14.3	0.339
Divertor region (incl. divertor plates)	8.3	0.5917
Total inboard (incl. divertor plates)	22.6	1.21

The maximum afterheat power density at the equatorial plane amounts to 1.1 W/cm^3 for the MANET at the first wall (4 % of the direct heating), to 0.285 W/cm^3 for beryllium (2 % of the direct heating) and to 0.396 W/cm^3 for the breeding ceramics (1.1 % of the direct heating).

2.4.4 Activation calculations

For calculating the activation the methodological approach developed for the afterheat calculation has been followed. In the activation calculation, however, it is mandatory to take into account material impurities and tramp elements to analyse their impact on the activation characteristics.

The following impurities have been used for beryllium [18] (in w%): 0.0512 O, 0.0435 Fe, 0.081 C, 0.025 Al, 0.025 Mg, 0.01 Si, 0.001 Zn, 0.006 Ni, 0.0085 Mn, 0.0005 Sc, 0.004 Cu, 0.0003 Ag, 0.004 Ti, 0.0004 Co, 0.002 Pb, 0.002 Ca, 0.001 W, 0.011 U, 0.002 Mo, 0.006 Cr, 0.038 N, 0.001 Zr. The NET material specification [19] for MANET-1 was assumed in the activation calculation for the steel (in w%): 0.13 C, 0.35 Si, 1.0 Mn, 0.005 P, 0.004 S, 10.5 Cr, 0.85 Ni, 0.75 Mo, 0.20 V, 0.15 Nb, 0.03 N, 0.05 Al, 0.008 B, 0.02 Co, 0.02 Cu, 0.09 Zr. For Li_4SiO_4 the following impurities were assumed [3] (w%): 0.158 Al, 0.104 C, 0.02 Ca, 0.008 Cr, 0.0005 Cu, 0.019 Fe, 0.020 K, 0.0049 Mg, 0.085 Na, 0.001 Ni, 0.01 S, 0.02 Pt, 0.0071 Ti, 0.0007 Zn, 0.0073 Cr. Numerical results of the activation analysis are given in Section 6. For detailed results see H. Tsige-Tamirat and U. Fischer [15]. Only some outstanding features are discussed in the following.

The activation behaviour of the MANET steel in the blanket is not significantly affected by impurities. This holds for the activation inventory, the contact γ - dose rate and the radiological hazard potential. For both beryllium and Li_4SiO_4, on the other hand, the contact γ - dose rate and the radiological hazard potential are dominated by activation products of impurities, whereas the activation inventory is dominated by the tritium content. In addition, there is an impact of secondary charged particle induced reactions on the activation properties of beryllium and Li_4SiO_4, see e. g. Tsige-Tamirat [20].

2.4.5 Irradiation effects on blanket materials

Neutron induced radiation damage was calculated for the MANET first wall, beryllium and Li_4SiO_4 at the equatorial plane of the outboard side of the DEMO-reactor, i. e. at its highest loaded part. The SPECTER damage code [21] along with its ENDF/B-V based data library was applied for this purpose. For beryllium, more advanced damage cross-sections were used, based on ENDF/B-VI recoil spectra for the contributing reaction channels and an improved method for calculating the damage energy [22]. The neutron spectra used to collapse the damage cross-sections were provided by a three-dimensional MCNP calculation in the SPECTER 100 energy group structure. For an integral operation time of 20000 hours the resulting maximum radiation damage amounts to 69.5, 20.3 and 29 dpa for the MANET, Li_4SiO_4 and beryllium, respectively.

The maximum helium production in beryllium is 16300 appm, and the maximum tritium production 208 appm. The peak fast neutron fluence ($E > 1.0$ MeV) is 2.55 x 10^{22} cm^{-2}. The maximum tritium production rate in Li_4SiO_4 is 3.57 x 10^{13} atoms $cm^{-3}s^{-1}$. The total tritium production is 382 and 3.14 g/d in Li_4SiO_4 and in beryllium respectively. The peak ^6Li burn-up is 7.25 at % referred to Li_{tot}. Due to the low ^6Li-enrichment of 25 at % the ^6Li burn-up is nearly constant across the first 20 cm of the Li_4SiO_4 pebble bed. The burn-up effect on the TBR has been assessed by performing a Monte Carlo calculation with the proper end-of-life (20 000 h) ^6Li-inventories. A TBR-reduction of 0,02 was obtained.

2.4.6 Shielding efficiency

The shielding performance of a breeding blanket in general is poor. Sufficient shielding has to be provided by material components arranged between the toroidal field (TF) coil and the blanket: the vacuum vessel and the back of the blanket segment. At the inboard side radiation shielding is most crucial. There

the totally available space amounts to 115 cm. The thickness of the vacuum vessel, acting as major shielding component, is 30 cm; 85 cm are left for the blanket segment. Actually 59 cm need to be used for the helium-cooled solid breeder blanket including 24 cm for the helium supply lines at the back of the blanket. Therefore, 26 cm of the space available for the blanket can be used for providing additional shielding.

Detailed three-dimensional shielding calculations have been performed for the previous version of the helium cooled solid breeder blanket [3]. It has been shown that the required radiation design limits for the TF-coil can be met for an integral operation time of 20.000 hours by applying different technical measures for improving the shielding efficiency, e. g. by inserting an efficient neutron moderating material at low volume fractions (20% ZrH) into the blanket back shield. In order to meet the required radiation design limits for an integral operation time of 10 years a larger volume fraction of an efficient neutron moderating material (e. g. ZrH or water) has to be inserted into the blanket back shield. Alternatively, the vacuum vessel itself can be optimised for ensuring a sufficient shielding efficiency.

2.5 Thermomechanical Analysyis

Ref. [23] and [24] illustrate in detail the methods and the results of the thermohydraulic and mechanical stress calculations. Here, it will suffice to recall the groundrules used for the calculations and the obtained results.

2.5.1 Calculation groundrules

The groundrules can be summarized as follows:

1. The convective heat transfer coefficient between coolant channel walls and flowing helium has been calculated using the correlation of Ref. [25]. The relevant thermohydraulic properties of helium are taken from the correlations proposed in Ref. [26].

2. The effective thermal conductivity of the bed of Li_4SiO_4 pebbles has been measured at KfK. For the bed of 0.3 - 0.6 mm Li_4SiO_4 in helium the measured effective thermal conductivity data may be correlated by the equation k_e [W/mK] = $0.708 + 4.51 \times 10^{-4} T + 5.66 \times 10^{-7} T^2$ with T in degree centigrades [27]. The heat transfer coefficient between pebble bed and containment wall is equal to 0.6 W/cm^{2}K according to the Schlünder correlation [28].

3. The effective thermal conductivity of the binary beryllium bed (1.5 - 2.3 mm and 0.08 - 0.18 mm beryllium pebbles) has been obtained by interpolating the experimental results of similar beryllium and Li_4SiO_4 pebble beds [27]. The used correlations are:

$$k_e\,[W/mK] = 6.235\left\{1+353\left[\alpha_{Be}\,(T_m - T_o) - \alpha_{Ma}(T_{Ma} - T_o) + \left(\left(1+\frac{\Delta V}{V}\right)^{1/3} - 1\right)\right]\right\}$$

$$\alpha\,[W/m^2K] = 3308\left\{1+383.1\left[\alpha_{Be}(T_m - T_o) - \alpha_{Ma}(T_{Ma} - T_o) + \left(\left(1+\frac{\Delta V}{V}\right)^{1/3} - 1\right)\right]\right\} \times$$

$$\times\left[1 + 9.239\times10^{-4}\,T_W\right]$$

where: k_e [W/mK] = effective thermal conductivity of the bed

α [W/m²K] = heat transfer coefficient between pebble bed and containment wall

T_m [°C] = average temperature of the pebble bed

T_o [°C] = temperature at which the bed filling operation has been perfomed ≈ room temp.

T_{Ma} [°C] = average temperature of the bed containing wall of MANET

T_W [°C] = local wall temperature

α_{Be} [K^{-1}] = thermal expansion coefficient of beryllium at T_m [29]

α_{Ma} [K^{-1}] = thermal expansion of MANET at T_{Ma} [29]

$\Delta V/V$ = volume swelling of beryllium under neutron irradiation

For the present calculations the Beginning Of Life (BOL) situation has been considered where the highest pebble bed temperatures are expected, thus $\Delta V/V = 0$. Section 7 shows how the effect of $\Delta V/V$ has been evaluated. Furthermore in the present calculation the term in T_w for the calculation of the wall heat transfer coefficient α has been neglected to simplify the calculations. This term has not a large effect on α and in any case it is pessimistic to neglect it.

4. The pressure drops in the helium systems have been calculated on the base of Ref. [30].

5. The radial and poloidal power distribution has been obtained by the three-dimensional neutronic calculations (Section 2.4). To obtain a uniform helium outlet temperature, the helium mass flow per blanket poloidal section has been assumed proportional to the power produced in the section itself. This means that the helium flow to each section should be controlled

by proper gagging. The same holds for the groups of parallel channels in the cooling plates used to cool the pebble beds.

6. The temperature and stress calculations have been performed with the FE computer code ABAQUS [31] and compared with the ASME code [32, 33]. The tridimensional FE mesh was generated using the CAD system BRAVO 3/GRAFEM. The properties of MANET are from Ref. [29] and [34].

2.5.2 Results

Detailed temperature and pressure drop calculations have been performed for the part of the blanket where the highest power densities are expected. These occur in the outboard blanket poloidal section at the equatorial plane of the torus. Furthermore the heat flux from the plasma to the first wall (FW) has been taken equal to the maximum specified value of 50 W/cm^2 (Section 2.1).

The temperature calculations have been performed for a radial-toroidal section with a poloidal height of six FW coolant channels corresponding to four blanket coolant plates (Fig. 2.5.1). The opposite directions of the coolant helium flow and the resulting helium temperature differences at the radial-toroidal boundary surfaces of the model have been accounted for by an iterative adjustment of the temperatures of these surfaces.

Fig. 2.5.1 shows a poloidal radial section of the F.W. and of the front part of the breeding region with the highest temperatures. The maximum temperature in the MANET structural material is 520 °C, which is lower than the recommended limit of 550 °C, where the mechanical properties of MANET start to decrease considerably. The maximum temperature in the Li_4SiO_4 pebble bed of 907 °C is well below the temperature limit of 1024 °C dictated by considerations of lithium transport (Section 6). In any case, even if this limit were reached locally, this would not have very severe consequences as this would entail that 1 ‰ of the lithium is removed from the affected blanket region at 1024 °C during the total blanket life of 20 000 hours. The maximum temperatures at the interfaces beryllium/MANET and Li_4SiO_4/MANET are 500 °C and 550 °C respectively, both well below the compatibility limits (Section 7 and 6). The maximum BOL temperature in beryllium is 637°C. The beryllium temperatures are important for the assessment of the beryllium swelling (Section 7).

The pressure drop in the helium coolant system between the inlet and the outlet at the top of the blanket segment is 0.3 MPa (Fig. 2.1) [23].

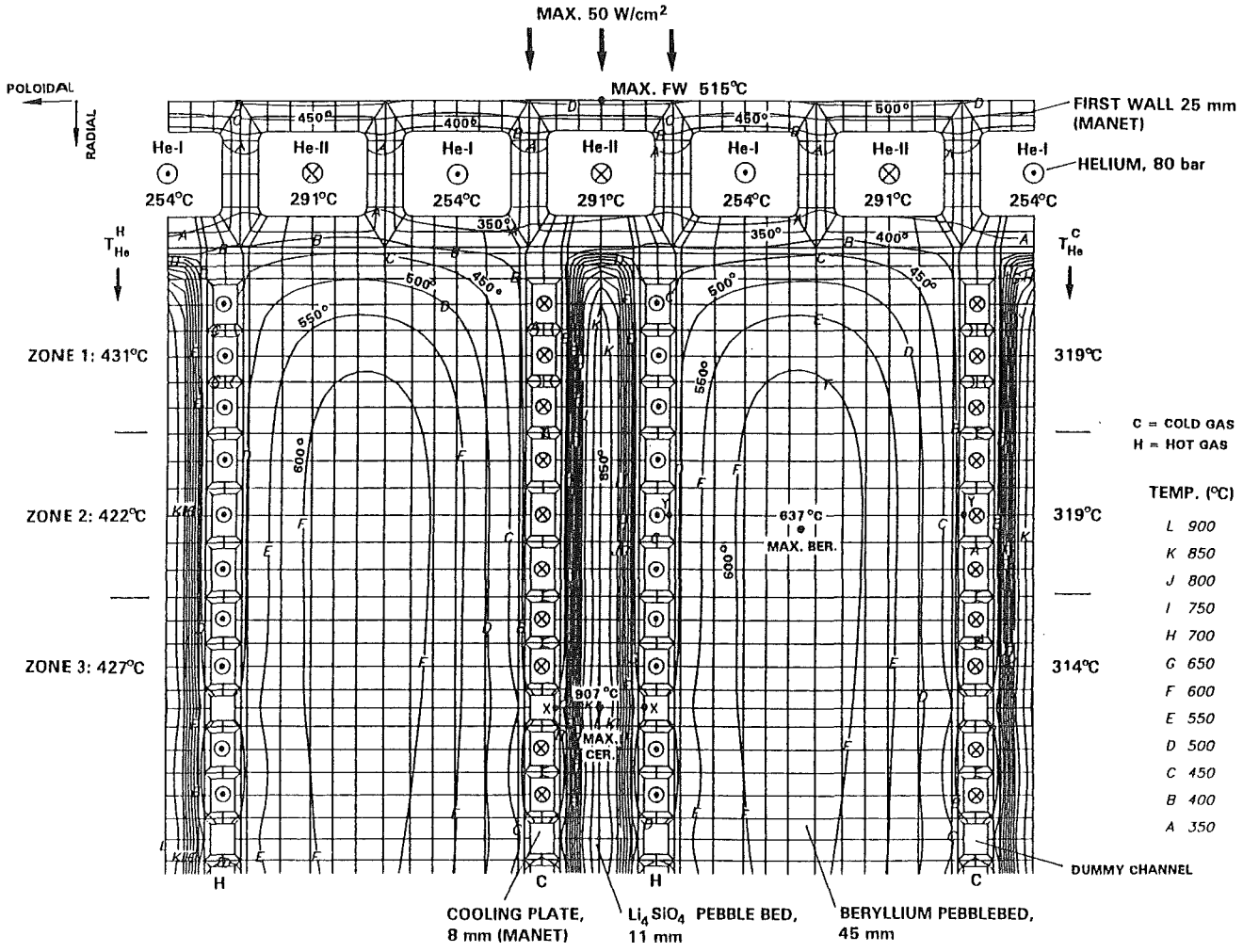

Fig. 2.5.1: Radial-poloidal section of the FW and blanket in the front part of the outboard blanket at the torus equatorial plane.

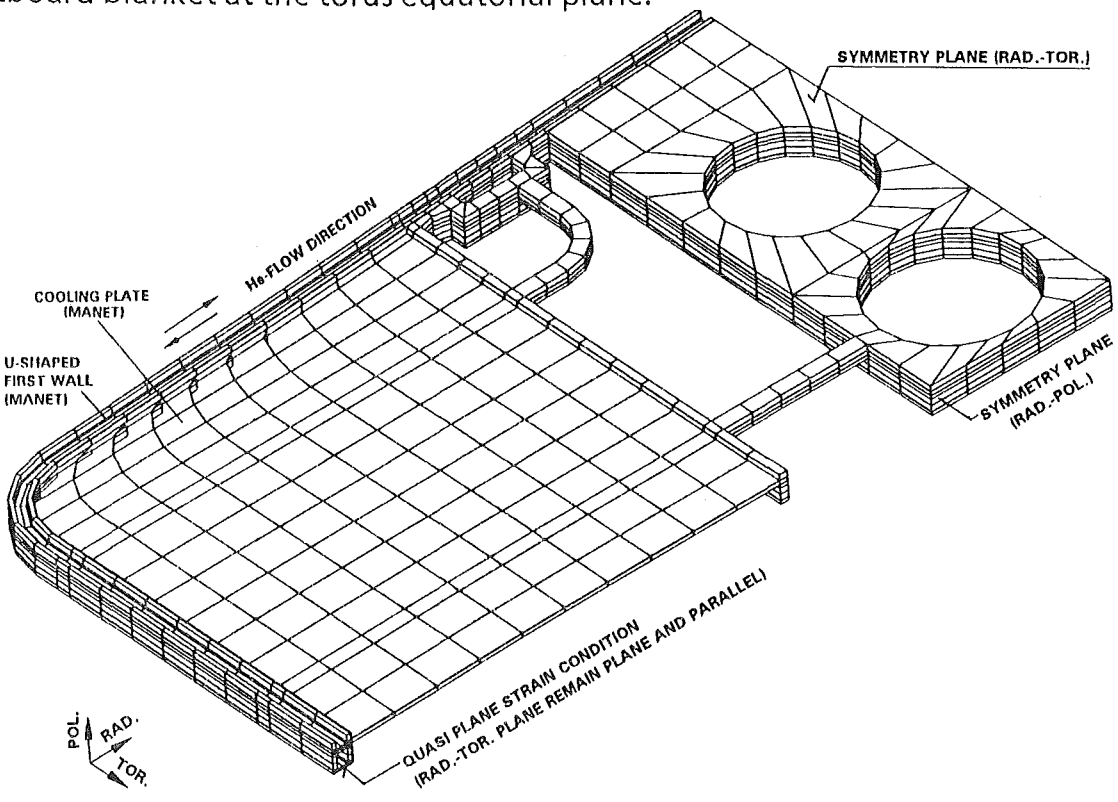

Fig. 2.5.2: Isometric view of a poloidal portion of the outboard blanket used for the FEM calculations.

The stress calculations have been also performed for poloidal sections of the blanket. For these calculations the generalized plane-strain condition in the poloidal direction was applied to the model. This means that planes perpendicular to this direction remain plane and parallel. This allows to calculate the stresses in all three dimensions with an essentially three dimensional computation.

The calculations were performed in two stages. In the first stage, more detailed calculations were carried out for the poloidal section shown in Fig. 2.5.1 (however for the whole radial length of the blanket). In the second stage, a poloidal section with only one and half FW channel pitch was considered, however here also the back part of the blanket box was accounted for (Fig. 2.5.2). At the present stage, consideration of the back of the segment box and of shields is not necessary because these are approximately at the same temperature as the back plate of the blanket box, and the back plates are already much more rigid than the walls of the blanket box.

In the first stage the calculations were performed for a) normal blanket operation with 8 MPa pressure in the coolant channels and 0.1 MPa in the rest of the blanket region, b) operation with a leakage from a coolant channel, i.e. 8 MPa helium pressure also in the rest of the blanket. In the second stage only the case b) was considered. The results of the stress calculations can be summarized as follows:

1) First stage (primary stresses and local thermal stresses): the maximum von Mises primary, and primary plus secondary stresses (both in the FW region) are in normal operation 56 MPa (at 400 °C) and 311 MPa (at 500 °C), while in the operation with a coolant channel leak these values are 131 MPa (at 400 °C) and 361 MPa (at 500 °C) respectively. All these values are considerably lower than the ASME limits for MANET, i.e. 300 MPa (primary stress at 400 °C) and 494 MPa (primary plus secondary stress at 500 °C)

2) Second stage (primary stresses and global plus local thermal stresses): the primary stresses in the FW are the same as in the previous stage. The maximum primary stress of 258 MPa (at 300 °C) is located at the blanket side wall near the short poloidal manifold (but not in the welded region). This value is lower than the ASME limit of 341 MPa. The maximum primary plus secondary stresses in the FW and in the position of maximum primary stress are 332 MPa (at 520 °C) and 487 MPa at 300 °C respectively, against the ASME limits of 452 MPa and 681 MPa respectively.

Calculations for the inboard blanket have not been performed so far, because lower temperatures and stresses are expected, since the power densities and dimensions are smaller and the cooling helium pressure is the same (see Section 3).

3. Main Helium Coolant and Helium Purification Systems

The main helium coolant system is relatively similar to that of High Temperature Helium Cooled Reactors (HTR) and even more to that of a Gas Cooled Fast Reactor (GCFR) due to the high pressure and lower temperature of the helium in comparison of these values for the HTR, so that industrial experience is available for the design of these systems. The present conceptual design has been performed in collaboration between Siemens-KWU and KfK.

3.1 Main Helium Coolant System

The main helium coolant system and the reasons for the design choices are described in more detail in Ref. [35], here only a short description is given.

Fig. 3.1 shows a scheme of the helium cooling and of steam/water systems. The helium cooling circuits from the 48 outboard segments are connected to two headers to maintain the complete separation of the two independent cooling systems. Six helium lines are connected to each of the headers, each line being provided with its own blower and steam generator. Five of the lines are in operation while one line is kept in reserve for the case a replacement of a malfunctioning line is required. The same arrangement is adopted for the 32 inboard segments, however here only three helium lines are departing from the headers of each redundancy: two in operation and one in reserve. This allows to have blowers and steam generators of about the same size for the inboard and outboard lines. At variance with Ref. [35] also the helium coolant pressure in the inboard blanket is 8 MPa rather than 10 MPa. This decrease has been made possible by the choice of cooling plates in the blanket rather than tube coils, which reduces the pressure drop considerably. Thus the total pressure drop in the inboard helium coolant circuit is the same as in the outboard blanket, i.e. 0.4 MPa by an average helium pressure of 8 MPa. This allows to maintain, as in the outboard blanket helium circuit, the pressure head ratio in the blowers to 1.05, which is convenient for having single stage blowers [35]. Table 3.1 shows the mean characteristics of the helium coolant systems.

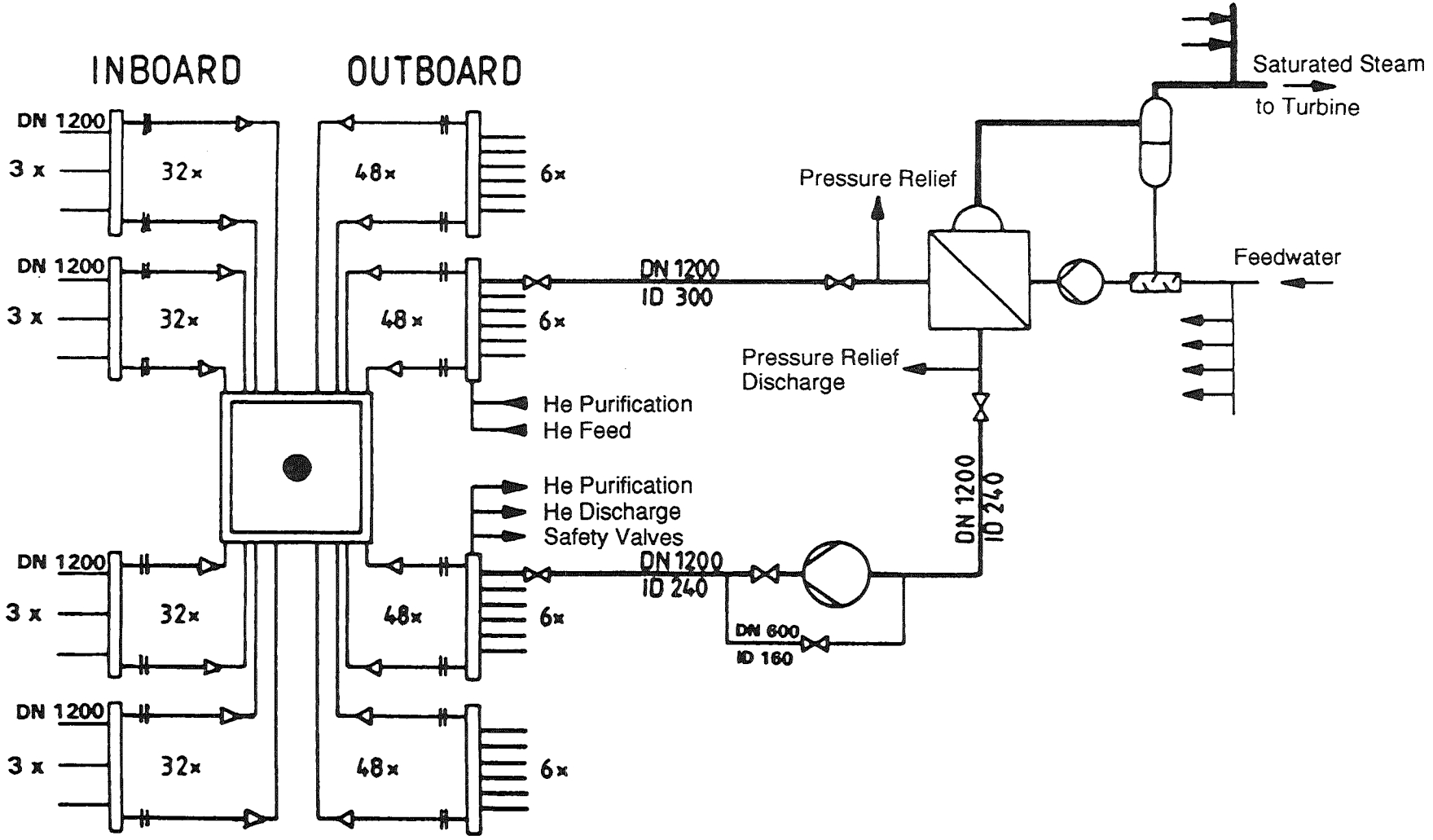

Fig. 3.1: Scheme of the main helium cooling and of the water/steam loops.

(◁ closing valve, ⋈ control valve)

In order to have no helium contaminated with tritium reach the water/steam side by a steam generator failure induced leak, the system pressure on the water/steam side has been chosen to be higher than the system pressure of the helium coolant circuits. Thus, the chosen steam pressure is 110 bar which corresponds to a saturated steam temperature of 318 °C. The layout of the water/steam system proposed by Siemens/KWU leads to a thermal efficiency of 34,64 %, which is higher than the minimum required in the DEMO specifications (Section 2.1). In the concept one separator flask, one mixing device and one circulation pump each are assigned to each steam generator (12 steam generators for the outboard, 6 for the inboard blanket segments). All steam generators deliver to one turbine [35].

Table 3.1 Main characteristics of the helium coolant system

		OUTBOARD	INBOARD
Volume of the cooling systems [m^3]		10 x 230.4 = 2304	4 x 236 = 944
Steam generators total surface [m^2]		30000	11000
Blanket power [MW]		1821	679
Coolant mass flow [Kg/sec]		1751	653
Helium coolant	inlet temp. [°C]	250	250
	outlet temp. [°C]	450	450
Helium average pressure [MPa]		8	8
Helium total pressure drop [MPa]		0.4	0.4
Blower pumping power [MW]		10 x 12.9	4 x 12.0

3.2 Helium Purification System

Helium is an inert gas. This offers great advantages. However, to make full use of them it is necessary to keep it very pure. Experience with helium cooled fission reactors shows that it is possible to keep it extremely pure, i.e. with a total amount of impurities less than 1 ppm [36]. This has been achieved by purifying continuously a certain fraction of the helium flow (slip stream fraction) to eliminate the small solid particles and the gas impurities. The impurities in the helium coolant

flow for the present blanket are expected to have less CO and more tritium than for thermal fission reactors, however in principle the helium purification system should be very similar. No attempt has been made so far to make a detailed design for the present blanket, however a conceptual design has been made for a test module of 3 MW power for a previous version of the present blanket [3], which is of course much smaller than the present blanket. However, this study has shown that purification is possible, without need of developing new techniques. In Ref. [3] it was assumed that the slip stream fraction is 0.1 % of the total coolant helium,The same assumption is made for the present design which means a slip stream mass flow of 2.4 kg/sec.

4. Tritium Control

The tritium control and the evaluation of tritium inventories are particularly important as the DEMO blanket has to show the capability of producing sufficient tritium for a continuous plasma operation by keeping relatively low tritium inventories and acceptable low tritium losses to the ambient. The main objective of the tritium control is to limit the tritium leakage from the helium coolant system to the water/steam cycle by permeation through the steam generator. The potential sources of contamination of the helium are the tritium permeation through the first wall and the walls separating the ceramic breeder and the beryllium from the helium coolant.

In the present design, the tritium control is based on a tritium purge flow system using helium plus 0.1 % hydrogen at atmospheric pressure to extract the major fraction of the tritium produced in the blanket. Furthermore, 0.1 % of the helium mass flow is continuously extracted from the main helium coolant circuit and sent to a helium purification plant for the extraction of the impurities and of the tritium coming by permeation from the purge flow or directly injected by the plasma into the first wall and then permeating to the main helium coolant system (Section 3.2).

The tritium permeation through the first wall and the tritium inventory in the first wall have been estimated using the DIFFUSE code to be between 1 and 100 g/d and between 3 and 300 g respectively [37]. Clearly, the upper value of permeation would make the tritium extraction more expensive as it would imply the extraction of tritium from the relatively large helium mass flow of 2.4 kg/sec. of the helium purification system (this problem would be much more severe with a water cooled first wall) and would cause a higher tritium partial pressure in the main helium cooling system and consequently higher tritium losses through the steam

generators. In any case, tritium in the helium purification system would not be lost, as it would be convenient to recover it, especially in the case of large quantities, with an extraction method similar to that proposed for the purge flow system (Section 5).

The tritium permeation through the first wall, a problem common to all the blanket concepts, depends mainly on the surface state of the first wall [37]. If, for instance, plasma sprayed beryllium, which at present appears to be the preferred solution of first wall protection, would be used, the recycle rate to the plasma of deuterium and tritium is very high and the resulting permeation to the coolant should be small [38]. In the present considerations the assumption is made that the permeation losses from the first wall are 1 g/d. The consequences of higher losses will be discussed.

The assessment of the tritium inventories and losses have been performed with methods illustrated in Ref. [39] and [3]. The tritium production quantities have been determined by neutronic calculations (Section 2.4). The permeation data for MANET are based on the experimental results of Ref [40].

Table 4.1 shows the main results of these calculations. As in Ref. [3], the tritium inventory has been calculated from the measured tritium residence time τ for the Li_4SiO_4 new reference pebbles (Section 6). The measured data can be approximated by the following equation:

$$\tau\,[s] = 0.2556 \times 10^{-2}\ e^{\frac{10835}{T\,[K]}}$$

where T is the local Li_4SiO_4 pebble temperature. The equation has been integrated between the maximum and the minimum temperature of the pebbles of 907 °C and 350 °C respectively applying the factor 1/3 [3].. Due account was also taken of the small pebble bed volume fraction (2 ‰) at temperatures between 300 and 350 °C.

The greatest tritium inventory is in the beryllium at the end of the blanket life (EOL). It was determined by the neutronic calculations minus the tritium released during the blanket operation, calculated with the code ANFIBE (Section 7).

The tritium purge system appears to be quite feasible. For the purge of the Li_4SiO_4 and of the beryllium pebble bed a helium flow velocity of 0.25 and 0.01 m/sec respectively have been assumed, which would imply a hydraulic resistance of the porous plate containing the beryllium pebble bed higher than that of the plate containing the Li_4SiO_4 one. This is probably necessary, as part of the beryllium pebbles are smaller than the Li_4SiO_4 ones and the pores in the plates have to

be smaller. The fixing of the helium purge flow velocities allows to calculate the tritium partial pressures in the two beds and thus the tritium losses to the main helium coolant system. In the calculations due account was taken of the dilution effect of hydrogen on the tritium permeation.

Table 4.1 Tritium inventories and control

Tritium inventories - in Li_4SiO_4 pebbles = 10 g - in the first wall = 3 to 300 g - in beryllium (EOL) = 1278 g - in solution in blanket structural material = 1 g - in the flowing purge helium (blanket region) = 0.077 g - in the main helium coolant system = 0.26 g
Tritium purge system - total purge helium mass flow = 0.65 kg/sec - average helium pressure = 0.113 MPa - purge helium velocity in Li_4SiO_4 bed = 0.25 m/sec in beryllium bed = 0.01 m/sec - pressure drop in Li_4SiO_4 bed = 0.0144 MPa outboard, 0.0078 MPa inboard - HT partial pressure in the purge helium (Li_4SiO_4 bed) = 1.33 Pa outboard, 0.69 Pa inboard - HT partial pressure in the purge helium (Be bed) = 0.06 Pa outboard, 0.035 Pa inboard - H_2/HT ratio: 85 outboard, 164 inboard
Tritium losses - direct loss from plasma to the main coolant system = 1 g/d - by permeation from the purge system to the main coolant system = 1.84 g/d - by permeation from the main helium coolant system to the water/steam circuit = 22 Ci/d (HT partial pressure in main coolant system: 0.134 Pa outboard, 0.132 Pa inboard)

The tritium losses to the steam generators have been calculated accounting for the losses into the main helium coolant system (blanket and first wall) and the effect of the helium purification system. The tritium permeation through the heat generators was determined with the same assumptions of Ref. [41], i.e. for preoxidized Incoloy 800. No account was taken for the beneficial effect of the tritium dilution caused by hydrogen. The so calculated tritium losses to the steam/water circuit of 22 Ci/d would probably be acceptable. However, a significant increase of the tritium permeation from the first wall above the assumed 1 g/d and the possibility of temperature transients, which can exert a temporarily detrimental effect on the oxide barrier of the steam generators surface [41] would imply the necessity of reducing the tritium losses to the steam/water system. Various possibilities have been discussed in Ref. [42], namely:

a) Development of an aluminizing system to reduce the tritium permeation through the walls of the helium/water-steam heat exchangers.

b) Development of an aluminizing system for the plates separating the breeder and beryllium from the main coolant system. In this case in-pile tests are required to investigate a possible degradation of the Al_2O_3 layer under irradiation, especially in presence of thermal stresses, and the compatibility with lithiated ceramics.

c) Development of a permeation barrier for the inner surfaces of the MANET first wall coolant channels.

d) Investigation of the necessity and/or possibility of maintaining an oxidizing atmosphere in the main helium coolant system to allow the selfhealing of the Al_2O_3 layer on the surface of the permeation barrier.

e) Development of catalyzers to promote the oxidation of HT to HTO in the main helium coolant system.

f) Investigation of the possibility of diluting the amount of tritium in the main helium coolant system with a certain amount of hydrogen and its effects on reducing the tritium permeation through the steam generators.

This work should be part of the further R&D program.

5. Tritium Extraction System (TES) for the Blanket Purge Gas [43]

Tritium is expected to be released in two chemical forms (HT and HTO) from the blanket zone. Therefore, two specific process steps are used for its recovery from the purge gas: freezing out of Q_2O (Q = H,T) in a cooler at 173 K, and adsorption of Q_2 on a molecular sieve (MS) bed at 78 K. This concept has been chosen after reviewing several TES proposals published for a NET/ITER solid breeder blanket. It is characterized by two main advantages:

a) Only a few components are exposed to the high gas flow rates of the primary purge gas loop; most of the gas processing and separation work is carried out in secondary loops where much smaller flow rates are applied.

b) The technical feasibility of the concept has been investigated with a positive result by an engineering company (Linde AG), who also provided a first layout of the primary gas loop for two alternative purge gas pressures.

The main TES requirements and design parameters are summarized in Table 5.1.

Table 5.1: Requirements and Design Parameters of the Tritium Extraction System

Tritium Production Rate[a)]	383 g/d = 63 mole T_2/d	
Mass Flow of Helium Purge Gas	0.65 kg/s = 5.8 X 10^5 mole/h	
Average Helium Pressure	p(He) = 110 kPa	
Swamping Ratio	He : H_2 = 1000 : 1[b)]	
Mass Flows and Concentrations	Purge Gas Component	
	TES Inlet	TES Outlet
He	14 x 10^6 mole/d	14 x 10^6 mole/d
H_2	14 x 10^3 mole/d	1400 mole/d
HT[c)]	101 mole/d	< 10 mole/d
HTO + H_2O[c)]	25 mole/d	0.2 mole/d
Impurities (N_2, CO, CH_4, ...)	< 5 mole/d	< 1 mole/d[d)]

a) Production rate = removal rate

b) With respect to the capacity of the MS beds and the U getter beds it would be desirable to have a ratio He : H_2 = 5000 :1 and a corresponding ratio of H : T = 41.9

c) It is assumed that tritium is released from the breeder material (Li_4SiO_4) in the form of gaseous HTO; the release rate is 126 mol HTO/day.

About 80 % of the tritiated water will be chemically reduced at the steel walls of the blanket; thus one gets 25 mol HTO/day + 101 mol HT/day; in addition, some of the HTO may be converted into H_2O by isotopic exchange

d) Some removal is necessary to avoid the accumulation of impurities

A simplified block diagram of the TES primary loop is shown in Fig. 5.1.

A precooler PC1 is used to cool the purge gas to 308K; the gas is then transferred to the main cooler C1, where it is further cooled to 173K. At this temperature, the Q_2O content of the gas is almost completely condensed and frozen out at the surface of the cooling tubes; the residual concentration is <0.015ppm.

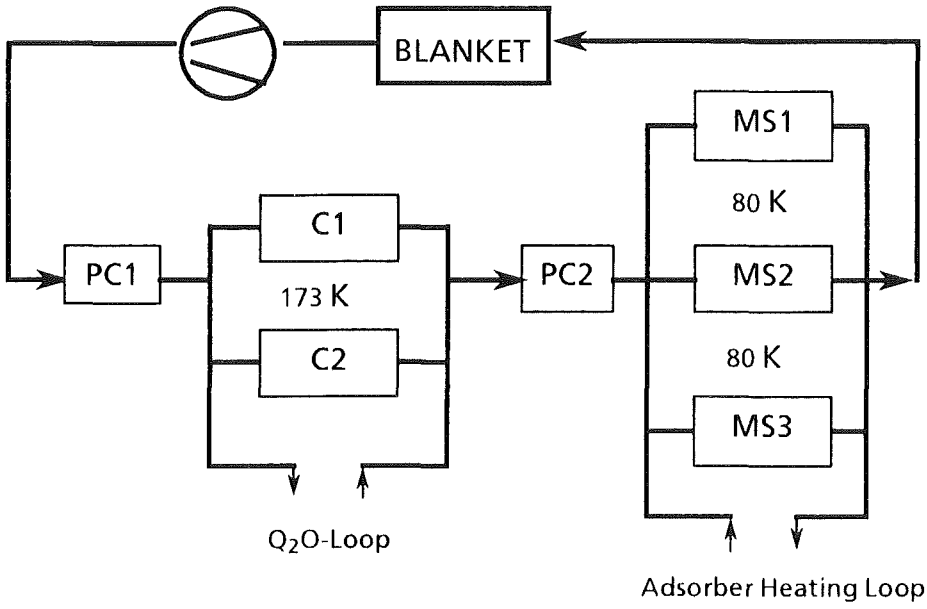

Figure 5.1: Block Diagram of the Tritium Extraction System

In order to prevent the accumulation of more than 100g tritium in the cooler C1, its operation time will be about 32 hours. The purge gas is then directed to a second cooler C2, while the ice collected in the first one is thawed. Recovery of tritium from the water molecules is carried out in a secondary loop (Q_2O-Loop) by using the water gas shift reaction and a Pd/Ag diffusor to separate the hydrogen isotopes from helium and CO.

Further processing of the primary purge gas is carried out by using the second precooler PC2 and three simultaneously operated 5A molecular sieve beds (MS beds); the operation cycle includes 3 steps:

1. Adsorption of hydrogen isotopes and gaseous impurities at 78 K,
2. Desorption of hydrogen isotopes and co-sorbed helium at $T \leq 160$ K,
3. Re-cooling to 78 K.

To enable steps 2 and 3, the MS beds are connected to an Adsorber Heating Loop, which additionally serves to separate Q_2 from He, and an Adsorber Recooling Loop. The operation time of each step is 6 hours; thus, the tritium inventory of the MS beds will remain below 100 g. Storage of the recovered HT/H_2 is carried out by using uranium getter beds in the Q_2O-Loop as well as in the Adsorber Heating Loop.

6. Li_4SiO_4 Pebbles

6.1 Introduction

Li_4SiO_4 has been chosen as reference material for the KfK BOT concept because of its high lithium density and fast tritium release. To reduce thermal stresses and thus to improve mechanical stability small pebbles are used. He + 0.1 vol% H_2 is used as reference purge gas to improve tritium release.

The blanket design imposes the following requirements:

1. Pebble density > 90 % TD to achieve a sufficiently large breeding ratio
2. Thermal stability: vaporization losses < 1 ‰ (2×10^4 h). This limits the maximum pebble temperature to < 1020 °C.
3. Mechanical stability: fraction of dust (< 10 µm) < 1 ‰
4. Compatibility with
   - austenitic and martensitic steel (limits the contact temperature to < 800 °C)
   - beryllium (limits contact temperature to <700 °C)
5. Tritium residence time < 10 d. This requires a minimum pebble temperature ≥ 300 °C.

These requirements must be satisfied for DEMO relevant irradiation conditions, which are characterized by

- pulsed operation (2×10^4 cycles, temperature change 300 °C, temperature rate of change of about 2-3 °C/s, in a few cases up to 30 °C/s)
- irradiation time 2×10^4 h
- lithium burnup 5 - 10 %
- damage 20 dpa

Very important parameters are the thermal conductivity of the pebble bed and the heat transfer coefficients between the pebble bed and adjacent walls because these determine the temperature distribution in the bed.

The data in the following are taken from the extensive status report prepared October 1991 [3], if not otherwise specified. Only newer work not contained in [3] is referenced.

6.2 Fabrication

6.2.1 Starting materials

Lithium orthosilicate (Li_4SiO_4) is readily available. The cost of powder is about 60$/kg. SiO_2 is very widely used in the ceramics industry. The cost is about 5 $/kg Typical purity levels of the powders are:

Li_4SiO_4: Al < 0.002, Na 0.070, K 0.028, C 0.564 wt%

SiO_2: Al < 0.021, Na 0.0026,, K 0.002, C < 0.007 wt%

The used enriched lithium was in form of Li_2CO_3 with 95.56 % ^6Li enrichment. Typical purity levels are: K 72, Na 123, Ca 507, Fe 20, Cu 35, Mg 30, Ba 10, Pb 4 (appm).

6.2.2 Fabrication process

The reference pebbles are fabricated by Glaswerke Schott by melting a mixture of Li_4SiO_4 and SiO_2 powder (in case of ^6Li enriched Li_4SiO_4 , a mixture of Li_4SiO_4, SiO_2 and ^6Li enriched Li_2CO_3 is used) and then spraying the liquid material. This procedure involves rapid quenching, thus some pebbles contain cracks and stresses. The pebbles have been optimized by KfK with respect to mechanical stability, but maintaining the excellent tritium release behaviour of Li_4SiO_4. The reference pebbles contain an excess of 2 wt% SiO_2 over the stochiometric composition. For the larger (0.3 - 0.6 mm ∅) pebbles the scatter in the mechanical stability is reduced by annealing at 1030 °C for 5 min and slow cool-down afterwards. This causes crystallization of Li_4SiO_4 and the remaining SiO_2 rich phase to precipitate thus filling the gaps at the grain boundaries and healing the microcracks. For the small pebbles (0.1 - 0.2 mm ∅) the mechanical stability is reduced by annealing, therefore they are used as produced. With a wind-sifting machine unround and hollow pebbles are separated.

The fabrication process is suited for a large-scale, reactor-relevant production. At the moment the firm Schott can produce 5 kg in 8 hours. A plant for the production of 30 - 40 tonnes per year is readily feasible. A detailed study with the aim to avoid cracks and thus the necessity of annealing the pebbles in the large-scale production is underway.

6.3 Li_4SiO_4 Pebble Characterization

Composition		Li_4SiO_4 + 2 wt% SiO_2	
Purity		Al 0.016, Ca 0.02, Fe 0.015, Na 0.011, C 0.1 wt%; Cr 17, K 54, Ni 19, Ti 42, Zn 8 [µg/g]	
Shape		Spherical	
Density	pebbles	97 - 98 % TD	
	bed	1.49 g/cm^3	
Porosity		≈ 100 % open	
Pebble diameter (mm)		0.3 - 0.6 (annealed)	0.1 - 0.2 (not annealed)
Grain size (µm)		20 - 40	< 1
Specific surface area (m^2/g)		1.3	--

6.4 Properties

Physical, thermal and mechanical properties for α-Li_4SiO_4, which is the relevant phase for blanket applications, have been compiled previously [29, 44]. Only pebble characteristics of fundamental importance for the design are discussed below.

Thermal stability, vaporization. The total lithium species vapor pressure is less than 10^{-2} Pa below 1120 °C [45] and the LiOH pressure is less than 10^{-2} Pa below 963 °C at 1 Pa water vapor pressure [46]. Li_4SiO_4 reacts with hydrogen under formation of water vapor and an oxygen-deficient surface layer. For the reference purge gas (0.1 % H_2) the total pressure of lithium bearing species is less than 0.111 Pa below 1024 °C [47]. This suggests that lithium transport is acceptably low below about 1024 °C because at this temperature the maximum lithium transport over the 20000 hours of the DEMO blanket operation time is less than 1 ‰.

Mechanical properties (fracture load). The fracture load characterizes the mechanical stability of the pebbles. It is an important parameter for the optimization of the fabrication route with respect to mechanical stability and to test temperature or irradiation induced changes in mechanical stability (Section 6.7). The conclusions concerning mechanical stability are mainly based on the results of thermocycling tests (Section 6.7).

Bed thermal conductivity and heat transfer coefficients. For all relevant bed configurations (Li_4SiO_4 pebbles, beryllium pebbles and mixed beds), the bed thermal conductivity and the heat transfer coefficients at the wall of the bed container have been measured and the data have been correlated by analytical expressions,

taking into account all important parameters [48, 27]. These experiments were generally performed in vertical test sections with pebble beds of about 50 cm in length. Although many experiments with large temperature differences between bed and container walls were performed, no fracture of pebbles, or indentations or thermal ratcheting effects on the container walls were observed.

6.5 Tritium Release

Large ($\approx$ 0.5 mm ∅), annealed pebbles of essentially all produced charges have been tested in purged inpile experiments. Small additions of SiO_2 and/or Al_2O_3 had only a minor influence on tritium release. Tritium residence times for these pebbles and for the reference purge gas (He + 0.1 vol% H_2) at 400 °C were 15 h for the "old" reference materials (stoichiometric Li_4SiO_4, Schott 86) [9], about 12 [50] and 7 h [51] for the "new" reference material (2 wt% SiO_2 surplus, Schott 89/3 and 90/6) and 24 h for Li_4SiO_4 plus 2 wt% SiO_2 and 1 wt% Al_2O_3 [50]. There is no indication that the residence time, i.e. tritium inventory increases with lithium burnup in the range up to 3 % [51].

A purged inpile test with small (0.1 - 0.2 mm ∅), not annealed pebbles and with mixed beds of small Li_4SiO_4 and beryllium pebbles with low lithium burnup has been performed and is being evaluated (CORELLI-2), a second test up and beyond to DEMO-relevant lithium burnup (10 %) is under irradiation (EXOTIC-7).

6.6 Compatibility

Out-of-pile tests of Li_4SiO_4 with austenitic steel 316L and with martensitic steel 1.4914 in presence of NiO (oxygen source) and of water vapor up to 100 Pa partial pressure (blanket purge gas $\approx$ 0.1 Pa), indicate an upper temperature limit of 800 °C [52]. Out-of-pile tests also showed that the maximum allowable temperature at the interface Li_4SiO_4/beryllium should be $\leq$ 700 °C [53].

The results of the purged SIBELIUS irradiation [54] are for Li_4SiO_4/beryllium and those of the closed capsule irradiation COMPLIMENT [55] are for Li_4SiO_4/steel in agreement with the out-of-pile tests.

6.7 Irradiation and High-temperature Behavior, Thermal Cycling Tests

Irradiation behavior. As mentioned, tritium release and compatibility are not affected by irradiation up to a lithium burnup of 2 - 3 %. Concerning the mechanical integrity of the pebbles the available results are somewhat contradictory [56]:

whereas in ALICE-3 (600 °C, burnup 2.7 %), SIBELIUS (270 - 470 °C, burnup 1.8 %) and in EXOTIC-6 (430 - 640 °C, burnup 3.1 %), the pebbles were intact after irradiation, in COMPLIMENT (400 - 450 °C, burnup 1.8 %) about 50 % decomposed into grain-size particles. This result, which was common to most of the other irradiated lithiated ceramics was attributed to temperature shocks caused by scrams of the OSIRIS reactor. Surprisingly the fracture load of intact pebbles from COMPLIMENT is essentially the same as that of unirradiated pebbles [57]. Irradiations in the fast reactor FFTF (BEATRIX-1) indicated that the pebbles remain intact up to 6 % lithium burn-up (80 % of the peak DEMO value). The now running EXOTIC-7 experiment will allow to assess the effects on pebble mechanical integrity for lithium burn-ups of 10 - 15 % which are considerably higher then the DEMO peak values.

High-temperature behavior. No decrease of fracture load was observed after heating dry, annealed large (0.3 - 0.6 mm ∅) pebbles at 800 °C for 1340 h [58] and dry, not-annealed small (0.1 - 0.2 mm ∅) pebbles at 650 °C for 1008 h. For pebbles containing water, the fracture load drops during the first hours of heating by 30 - 50 % until all water is released and stays then constant. Contact with beryllium did not influence the mechanical strength of the pebbles [27].

Thermal cycling tests. In tests with up to 1000 thermal cycles with unirradiated Li_4SiO_4 and mixed Li_4SiO_4/beryllium pebble beds no cracking of the beryllium pebbles was observed. The Li_4SiO_4 pebbles break independently of size only if the temperature change over the time exceeds a critical value, which depends on the pebble temperature [27, 59]. This limit is higher than the peak value expected for the DEMO blanket, as has been shown for the design with cooling coils [59] as well as for the present design [60]. Another important result of these experiments was that, although the bed was kept in place by a wire net with mesh size of about 50 µm, no broken particle was coming out of the bed although some broken parts were as small as 10 µm and the helium was flowing through the bed at velocities considerably higher than those foreseen in the Demo-blanket. Tests with Li_4SiO_4 pebbles irradiated to DEMO relevant burnup ($\approx$ 10 %) are in preparation.

6.8 Long-term Activation/Waste

6.8.1 Activation

Calculations. The calculated γ-activity of a pure silicate fusion blanket is about one or several orders of magnitude less than that of aluminate or zirconate blankets, respectively [61].

Measurements. Four years after the COMPLIMENT-HFR irradiation (Cd-screened, 178 FPD, lithium burnup 0.28 %, neutrons 1.29 dpa, α+t 0.08 dpa) the contact dose rate of Li_4SiO_4 pellets (the purity of the starting material is similar to that of the pebbles) was 24 μSv/hg and the most prominent γ-activities were (in Bq/g): Mn-54 2.7×10^3, Co-60 1.2×10^4 (both probably from capsule steel contaminations) and Zn-65 4.1×10^3 [56].

6.8.2 Reprocessing (recovery of Li-6 from irradiated breeder) and waste management

Reprocessing of the irradiated pebbles by melting is considered to be feasible. The process would consist in melting the irradiated pebbles with the proper amounts of Li^6 enriched Li_2CO_3 and SiO_2 and producing the pebbles in the usual way. The process should be considerably simpler and cheaper than in the case of sintered pebbles where the formation of very fine powder for the sintering process is required [62]. The firm Schott has produced Li_4SiO_4 pebbles by remelting Li_4SiO_4 pebbles (charge 90/6). These pebbles have practically the same mechanical properties and tritium release characteristics as the usual pebbles.

By the Schott production method a material efficiency of 85 % (ratio between pebbles weight and initial powder weight) is achievable [63], so that, by every reprocessing operation, about 15 - 20 % of the Li_4SiO_4 would not be reused. This quantity would require a disposal. The activity of this material would not be very high, as the tritium would be eliminated during the melting process and the activation is extremely low. However, probably the reprocessing would require remote control [62]. The waste disposal aspect has not been so far investigated in detail. It should, in principle, not pose very difficult problems [62].

7. Beryllium

Beryllium is a very effective neutron multiplier. Solid breeder blankets with lithiated ceramics as breeder and steel as structural material require beryllium to obtain a tritium breeder ratio higher than one.

In the present design the beryllium is used in form of small pebbles. This offers various advantages. Under neutron irradiation beryllium becomes brittle and swells. Within small pebbles the temperature differences in the pebble are small, thus the stresses caused by thermal gradients and by different swelling rates (swelling is temperature dependent) are considerably smaller.

7.1 Pebbles Fabrication

Two kinds of beryllium pebbles form the pebble bed placed between two cooling plates of the blanket (see Section 2.2). The main structure of pebble bed is given by the larger pebbles (1.5 - 2.3 mm in diameter) with a packing factor of 63.3 %. In the space between the larger pebbles there are smaller beryllium pebbles (0.08-0.18 mm in diameter) with a packing factor of 17.5%

Both kinds of pebbles are fabricated by melting. The larger pebbles are a by-product in the metallic beryllium production method of the firm Brush-Welman and thus relatively cheap. The smaller pebbles are produced by Brush-Welman either by the rotating electrode method (REP) or by melting and spraying with an inert gas. Table 7.1 shows the main characteristics of the two kinds of pebbles.

Table 7.1

	Pebble diameter [mm]	Closed porosity	BeO content	Other impurities [ppm]
Large pebbles	1.5 - 2.3	0.57 %	0.3 %	Fe 520, Al 345, Mg 1200, Zn 85, Ni 85, Cu 25, Co 8, U 125, Cr 105, Zn 210, N 215
Small pebbles (REP fabricat. method)	0.08 - 0.018	0.86 %	0.08 %	Al 250, Mg 250, Ni 60, Cu 40, U 110, Cr 60, N 380, Fe 435

7.2 Compatibility

Out-of-pile tests show that the compatibility limit between beryllium and Li_4SiO_4 is 700 °C [53], and for beryllium/316L steel and beryllium/MANET, the limits are 580 °C and 650 °C respectively [64]. The results of these out-of-pile experiments have been confirmed by the SIBELIUS irradiation performed in a thermal reactor at 550 °C for 200 hours with a He + 0.1 % H_2 atmosphere [54].

7.3 Behavior of Beryllium under Irradiation

The behavior of beryllium under irradiation, particularly with respect to swelling, embrittlement and tritium release, is probably the key issue for the solid breeder blankets. Swelling of the beryllium results from the helium produced by the (n, 2n) reaction while tritium is produced by secondary reactions.

7.3.1 Beryllium swelling

As the results of in-pile irradiations at high temperatures are rather scarce, irradiations were performed in the thermal reactor SILOE /Grenoble, in the temperature range 240 - 700 °C and for neutron fluences of 2 - 2.5 x 10^{21} cm^{-2} ($E_n \geq 1$ MeV) corresponding to helium contents of 1100 - 1400 appm (BEGONIA experiment) [65]. These fluences are of course considerably smaller than the peak values expected in the present design (16300 appm helium), therefore irradiations are planned in the fast reactor Phenix to begin at the end of 1994.

As the swelling data for the peak neutron fluences of the present blanket are not yet available, modeling work on helium behaviour in irradiated beryllium has been initiated by KfK. A rather sophisticated computer code (ANFIBE) has been developed. This code describes the precipitation of helium atoms into intragranular bubbles, the migration of these bubbles to the grain boundaries to form intergranular bubbles, the growth and coalescence of these bubbles and their interlinkage with pores. The description of the helium behavior in beryllium accounting for the beryllium properties (mainly surface tension, temperature and irradiation induced creep) allows to calculate the volume swelling. The comparison of the ANFIBE calculations with the experiments available from the literature, including the BEGONIA experiments, both at low and at high temperatures shows an excellent agreement [66]. The experimental data covers independently the ranges of temperatures, fast neutron fluences and helium contents for the present blanket. However, more data are required to qualify ANFIBE especially

from experiments in which irradiations to high fluences have been carried out at high temperatures.

Fig. 7.1 shows the swelling of the beryllium pebbles calculated with the ANFIBE code for various temperatures and neutron fluences. The swelling of the beryllium pebbles causes a strong increase of the bed thermal conductivity so that the EOL peak beryllium temperature calculated by the ANFIBE-code is reduced from the BOL value of 637 °C (Section 2.5) to 500 °C and the resulting EOL maximum beryllium swelling is 8.3%. The initial space available for the helium flow to purge the tritium released from the beryllium is 20 % of the bed volume, so that sufficient space is available up to the EOL situation as well.

7.3.2 Beryllium embrittlement

First experiments were performed with unirradiated beryllium pebbles at room temperature. The larger pebbles were subjected to compressive tests. The pebble diameter could be reduced of up to 13% without formation of cracks.

The irradiation-induced embrittlement is very difficult to model and irradiation experiments are essential. However, contrary to swelling, beryllium embrittlement is produced at relatively low fluences which can be easily achieved in thermal test reactors. An European collaborative program to investigate the irradiation embrittlement of beryllium has been initiated; it involves the exposure of tensile, disc compact tension and transmission electron microscope specimens to a fluence of 1.5 x 10^{21} cm^{-2} ($E_n > 1$ MeV) at temperatures of 200°, 400° and 600 °C in the BR2 reactor at Mol.

The irradiation has been started in August 93 and has been terminated in March 1994. The results of the PIE work will be available at the beginning of 1995.

7.3.3 Tritium release from beryllium

Work on out-of-pile tritium release from beryllium irradiated in the SIBELIUS experiment has been started at KfK [54]. Further work on out-of-pile tritium release is being performed at KfK with beryllium irradiated at low temperatures and high fluences (1 - 4 x 10^{22} cm^{-2}, $E_n \geq 1$ MeV) in the BR2 reactor. Similar experiments will be performed with beryllium from the BR2 embrittlement experiment, from a recently started irradiation experiment in HFR and from the Phenix irradiation.

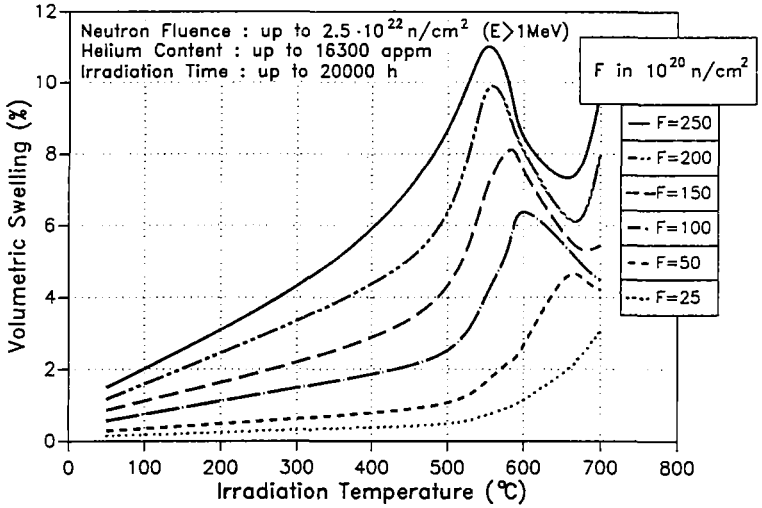

Figure 7.1: Beryllium pebbles volumetric swelling versus temperature at various fast neutron fluences for the BOT DEMO blanket as predicted by ANFIBE.

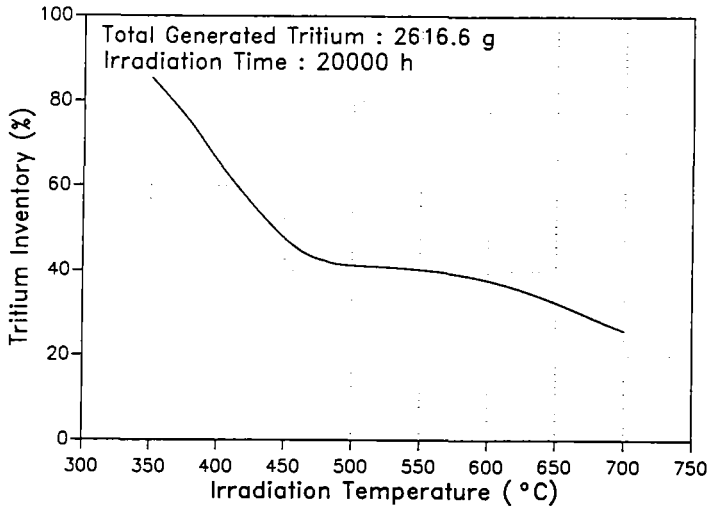

Figure 7.2: Tritium inventory at the BOT blanket end of life (EOL) versus beryllium temperature.

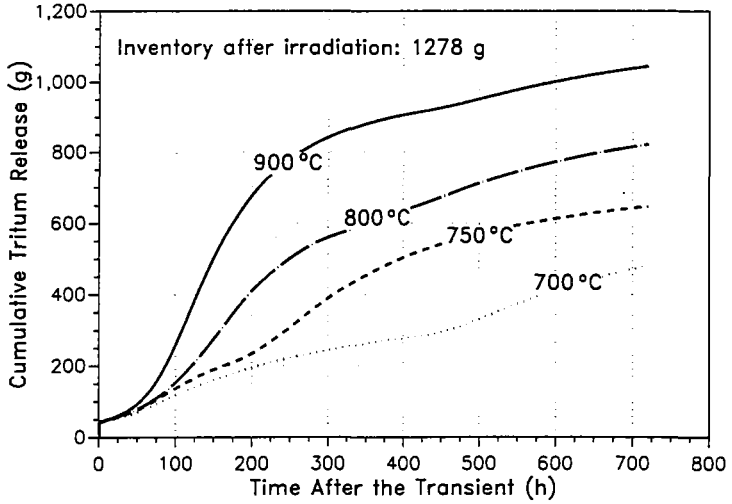

Figure 7.3: Cumulative tritium release from the beryllium pebbles after a temperature increase in 30 sec. up to the shown temperature. Afterwards the temperature remains constant at this value.

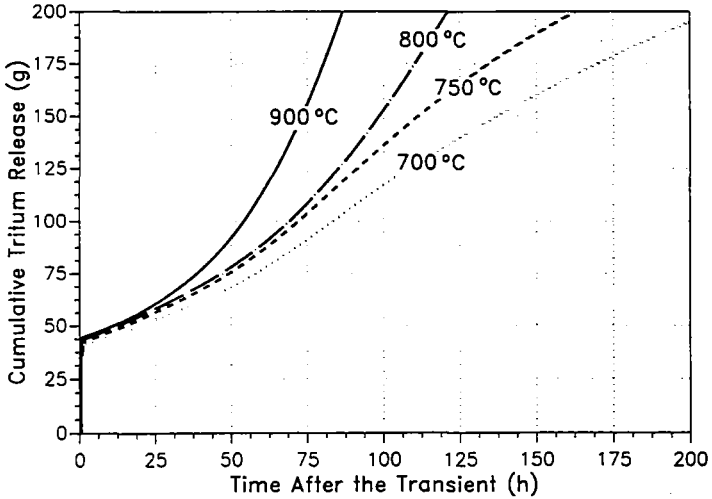

Figure 7.4: Cumulative tritium release by temperature increase. Detail for the first hours.

The results of these experiments cannot be directly applied to calculate the tritium inventory in the DEMO blanket. Therefore it was decided to extend the code ANFIBE for the calculation of the tritium release from beryllium. The diffusivity of tritium in beryllium is much higher than that of helium, but the tritium release is hindered by the helium bubbles (physical trapping) or by the beryllium oxide impurity (chemical trapping). The model describing the behavior of tritium is formally identical to that of helium, however, a rate-equation has been added, which accounts for the chemical trapping of the tritium by the oxygen impurities.

The comparison of the ANFIBE calculations with the experiments of Ref. [54] and other experiments from the literature [67, 68] shows a good agreement especially at higher temperatures [69]. However, more extensive experimental data, particularly with respect to in-pile tritium release, is required to qualify the code.

Fig. 7.2 shows the percentage tritium inventory remaining in the beryllium at the blanket end of life as calculated with the ANFIBE code. Of the total tritium produced in the blanket during its life, i.e. about 2600 g, the half is released and carried away by the helium purge flow. Figs. 7.3 and 7.4 show the tritium release which could occur during an overheating accident at the end of the blanket life when the tritium inventory in beryllium is the highest. After an initial burst release of about 40 g of tritium, the release is relatively slow.

8. Mechanical Behaviour During Disruptions

One of the crucial problems in the blanket design is to demonstrate the capability of the structure to withstand the mechanical effects of a major plasma disruption. In fact, in all operating tokamaks it has been observed that, under certain circumstances, the plasma collapses and the plasma current decreases very rapidly to zero. The rapid current variation produces induced eddy currents in the surrounding metallic structures. These currents, in presence of the strong stationary magnetic fields, produce large magnetic forces.

In order to compare the performances of different designs, the Test Blanket Advisory Group (1990) gave the following specifications for a reference disruption in DEMO: "a linear decay of the plasma current from 20MA to zero in 20ms" and "one disruption during blanket segment life". The only mechanical requirement was that "the blanket segment may be deformed but it must remain removable through the port".

On the basis of these specifications an assessment of the blanket structure (outboard and inboard segment box) has been performed. Some results of this assessment have been already presented [70, 71, 72], but a detailed description of methods and results will be published by the end of 1994 [73].

8.1 Electromagnetic Analysis

The electromagnetic calculation of the eddy currents and of the resulting magnetic forces has been performed by means of a 3-D finite element method (FEM) code commonly used for NET/ITER applications [74]. This code cannot take into account the magnetic properties of the steel MANET; the magnetic permeability of the material is assumed to be the vacuum permeability.

As a FEM model of the Demo reactor has been achieved, all the most relevant parts of the electromagnetic system can be taken into account in the calculation. The vacuum vessel, the 48 outboard and 32 inboard blanket segments as well as the PF-coils are part of the developed model. Particularly, a fine discretization of the outboard and inboard blanket segments has been realized to account for the complex design of the components. The presence of a plasma stabilizer ("saddle loop") attached to each outboard blanket box has been considered as well.

Fig. 8.1 shows the time behaviour of the induced eddy currents by the reference disruption. The vacuum vessel current flows in toroidal direction around the plasma torus. As each blanket segment is electrically insulated from the other segments and components of the reactor, the blanket current flows inside the segment closing a loop through first wall, side wall and back wall. The maximum current is reached at the end of quench (20 ms), then it decays according to the time constant of the different components (about 100 ms for the vacuum vessel and 10 ms for the blanket segments). The resultant forces acting on the blanket structures show a similar time behaviour. Fig. 8.2 shows the resultant forces and torques on the structure for different horizontal sections at end of quench. Very strong moments (see bending in toroidal direction and torque with respect to the torus axis on the section C) arise which are responsible for the highest stresses.

The effect of the magnetic steel MANET on the forces has been investigated. Because it is used as structural material in the region surrounding the plasma, the magnetic flux distribution outside and inside the blanket structure can be significantly modified. When a plasma disruption occurs, as eddy currents are induced in the structure, electromagnetic forces arise whose magnitude can be greater than in the case without ferromagnetic structural material.

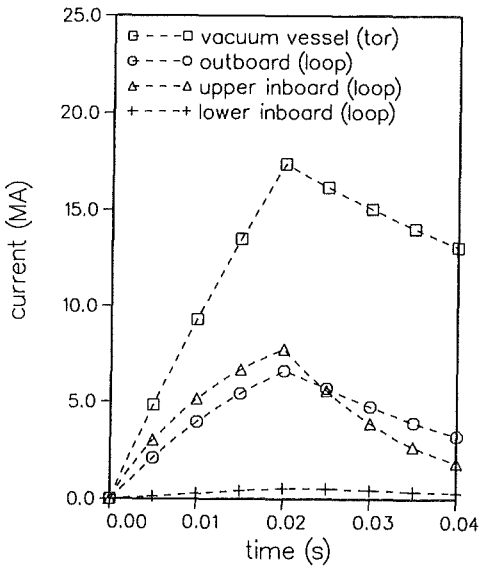

Fig.8.1: Time behaviour of the eddy currents for vacuum vessel and blanket boxes.

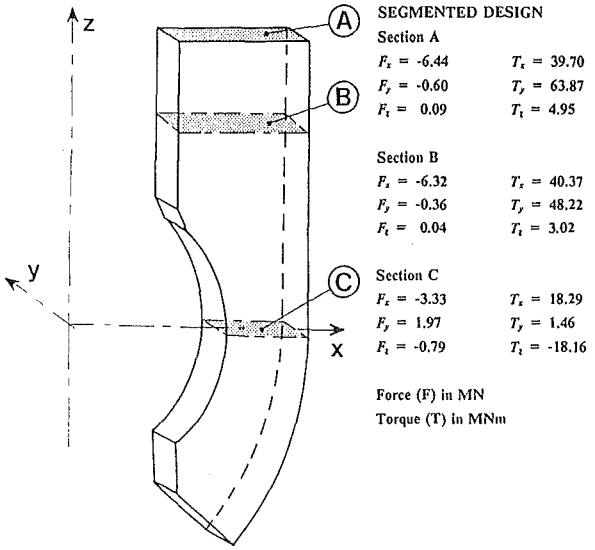

Fig.8.2: Load condition at quench end. Resultant forces and torques refer to the lower half in wich the structure is cutted by the reference plane (A,B or C). The torquesare calculated on the geometrical center of each reference section.

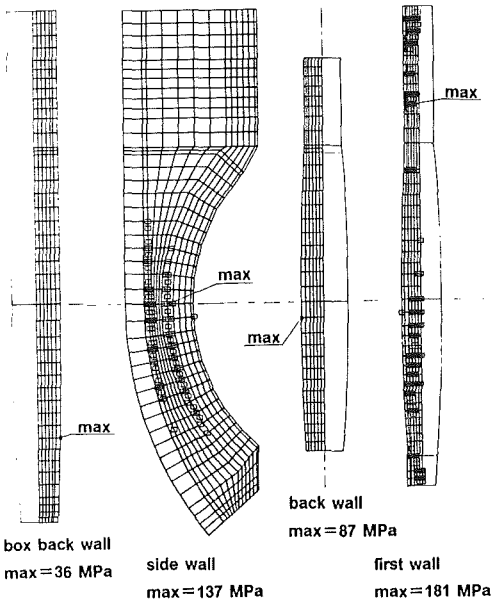

Fig.8.3: Von Mises stress distribution for the outboard blanket box.

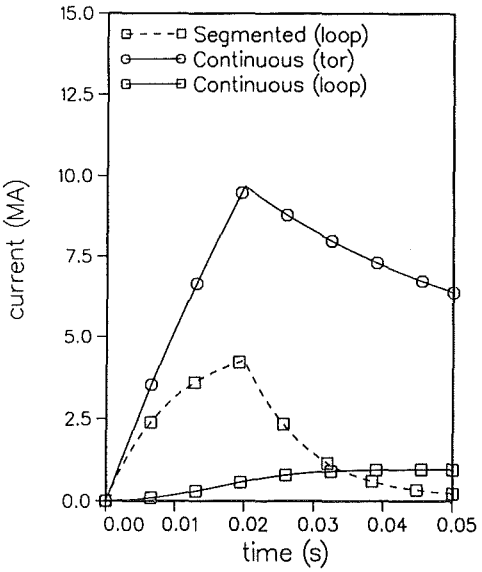

Fig.8.4: Eddy current in the continuous and segmented design.

A computer code that allows electromagnetic calculations in presence of saturated magnetic materials, is being developed [75]. Analyses performed with this new program for DEMO conditions show that forces in presence of magnetic structural material mostly change only their module values but not their direction. The largest increase of module values occurs for the box back wall and the vertical shield. However, this increase is limited to 20% in the first wall of the box, where the largest forces are acting and the highest stresses are expected. These results justify a factor of 1.2 used at the moment to increase the calculated magnetic forces accounting for the magnetic properties of MANET.

8.2 Stress Analysis

On the basis of the calculated force distribution, static and dynamic stress analyses of the outboard and inboard segments have been performed using the program ABAQUS [31]. Shell elements have been used to model the whole structure with the exception of the vertical shield where solid elements have been used (Fig. 8.3). As the first wall and the side walls are plates with internal cooling channels, anisotropic elastic material properties have been assigned for the corresponding FEM elements. The blanket boxes have been constrained (fully built-in) on the flange region. As the vertical shields of the 48 outboard and 32 inboard boxes are tied together to form two rigid toroidal shells, the support of neighbouring segments has been simulated by means of suitable boundary conditions on the vertical shield. Furthermore, the outboard blanket box is stiffened by 12 horizontal stiffening plates in order to provide stronger resistance against typical loads (bending and torque) due to plasma disruption.

Because of the mentioned constraints of the structure, the calculated displacements are relatively low. The maximum displacement (8mm) is less than the gap between adjacent boxes and between each box and the vacuum vessel (20mm). The maximum calculated von Mises stress lies considerably below the yield stress of the structural material at high temperature (560 MPa at 350 °C). Fig. 8.3 shows the von Mises stress distribution calculated by the static analysis of the outboard blanket box.

The results obtained by stress analysis have been assessed according to [32-33] taking into account the presence of thermal, pressure and self-weight loads acting on the structure. The total load caused by the reference disruption has been classified into Category 2 ("unlikely and design faults"). The results show that the outboard and inboard structures can withstand the mechanical stress caused by the reference disruption remaining below the elastic limit.

The martensitic steel MANET-I presents a degradation of the fracture toughness properties at irradiation temperatures less than 400 °C [76]. As the operating temperatures of the blanket structure are mostly in the range between 300 °C and 400 °C, a large amount of structural material is damaged by neutron irradiation. During the lifetime of the blanket, pre-existent cracks can grow due to cyclic loads such as thermal loads. Hence, the crack dimension can reach a critical value at which an unstable crack propagation is possible. Especially loads caused by plasma disruptions - in which a large amount of mechanical energy is deposited in few milliseconds into the structure - must be carefully considered in the calculation of the fast fracture limits [77]. Work on this problem is underway.

8.3 An Improved Design with First Wall Toroidal Connection

In order to reduce the mechanical impact of plasma disruptions a modified design concept ("continuous design") has been analysed [71].In the continuous design, a first wall electrical connection among neighbouring modules allows eddy currents to flow in toroidal direction. As the plasma stabilizing function is now performed by the continuous first wall, the presence of saddle loops is no longer necessary.

Fig. 8.4 shows the currents which flow in the outboard box. In the continuous design (CD) a large toroidal current is induced in the first wall; on the other hand the loop current remains relatively low due to the shielding effect of the toroidal current. In the case of the reference disruption, the loop current is reduced by a factor 4 in comparison to the corresponding current in the segmented design (SD). As the loop current is mostly responsible for the box structure load, the maximum stress is considerably reduced in the CD. On the other hand the toroidal current - although large - has a relatively low impact because it cannot produce large forces, due to the fact that the highest external field is also toroidal.

The CD presents great advantages in case of faster disruptions. Further calculations for disruption of 5 and 2ms show that the box structure can withstand the mechanical load produced in such events only in case of CD. In fact, the increase of the eddy current is limited by the greater time constant associated with the connected structure in comparison with the time constant of the SD.

8.4 Conclusions

The electromagnetic calculations and the stress analysis performed for the European B.O.T. Blanket demonstrate the capability of the inboard and outboard

blanket segments to meet the structural requirements for the Demo reference plasma disruption.

In this analysis a very detailed model of the electromagnetic system has been used. The magnetic properties of the steel MANET have been taken into account in the calculation by means of a new developed computer code.

As the toughness properties of the martensitic steel MANET degrade under irradiation, a fracture mechanics assessment for the components must be performed.

Finally, a continuous design has been analyzed. A comparison with the segmented design shows a better performance of the continuous design at least for centered disruptions.

9. Safety and Environmental Impact

This section presents the scope of hazard potential and accidents related to the blanket system as outlined in [78] under the following topics: (1) toxic inventories, (2) energy sources for mobilization, (3) fault tolerance, (4) release of radionuclides, and (5) waste management. The assessment includes the main components of the primary coolant system according to [35] and of the tritium purge gas system, but excludes auxiliary subsystems for storage, purification etc. which are not yet defined and will be subject to future analyses.

9.1 Toxic Inventories

Radioactive inventories in the different regions of the blanket (inboard, outboard, first wall, breeding zone, and manifolding plus shield region) as well as in the cooling systems have been assessed as described in Section 2.4 with supplemental information given in [79] and Section 4, and are summerized in Table 9-1 in two categories, i.e., tritium and activation products.

The tritium inventory in the breeder (Li_4SiO_4) has been calculated from the measured tritium residence time for the Li_4Si0_4 reference pebbles and is small (10 g). A considerable amount of tritium ($\simeq$ 3 g/d) will permeate into the primary helium coolant. This is assumed to be permanently removed via a 0.1 % by-pass flow branching off from the main cooling system. The assessment yielded a partial pressure of HT in the primary helium of approximately 0.13 Pa (corresponding to 0.3 g of tritium in 20000 kg of helium), provided that it is possible to extract continuously in the helium purification plant at least 90% of tritium from the helium slip stream fraction. The tritium losses to the steam circuit of 22 Ci/d were deter-

Tab. 9-1 Radioactive Inventories in Blanket and Related Systems

Blanket region or system	Tritium (g)	Activation Products after decay times (Bq)	
		0 s	1 year
Breeder material (Li_4Si0_4 w/o H-3)	10	$4.8x10^{18}$	$5.4x10^{14}$
Neutron multiplier (beryllium)	1278	$4.8x10^{19}$	$1.2x10^{18}$
Primary coolant (helium)	0.3	negligible	negligible
Purge gas (helium)	0.08	negligible	negligible
Tritium extraction system	300	negligible	negligible
Structural material (blanket segments)	12.1	$1.4x10^{20}$	$3.5x10^{19}$
First wall	5.5	$4.8x10^{19}$	$1.6x10^{19}$
Breeding zone	5.3	$6.3x10^{19}$	$1.5x10^{19}$
Manifold + shield region	1.3	$2.8x10^{19}$	$3.7x10^{18}$

mined with the same assumptions as in [41] (preoxidized incoloy 800 steam generator tubes with a barrier factor of 400). This value is close to the acceptable limit (Section 9.4). The losses would accumulate to 1.8 g of tritium in the entire water/steam system after 20000 h operation. The tritium inventory in the beryllium multiplier is the largest amounting to 1278 g at the end of the blanket life (Section 7). Release rates are discussed in Section 9.4. The tritium inventory in the purge gas is very small (0.08 g), however in the rest of the tritium extraction system the inventory amounts to 300 g. This is based on a preset limit of 100 g for each of the main components in the extraction system, i.e., the cold trap, molecular sieve, and uranium beds which seems to be achievable [80]. For the structural material the tritium build-up after 20000 h has been evaluated as 12.1 g, about half of which being in the first wall. This figure does not account for tritium permeating from the primary helium coolant and from the purge flow into the structure which is assumed to be benign.

Activation products inventories have been assessed for 20000 hours of full power operation. Typical specific activities for the blanket materials involved are compiled in Table 9-2 for different decay times. For the breeder the specific activity is comparably low when ignoring the small amount of tritium trapped in it. In the first wall structural material (MANET) the specific activities range

Tab. 9-2 Typical Specific Activites in Blanket Materials (Outboard)

Material / zone	Specific activity in Bq/kg after decay times of					
	0 s	1 h	1 d	1 month	1 yr	100 yr
Breeder (Li_4SiO_4 w/o H-3)	$9.2x10^{13}$	$6.8x10^{12}$	$2.1x10^{11}$	$3.9x10^{10}$	$1.0x10^{10}$	$3.0x10^{8}$
Multiplier (beryllium)	$2.1x10^{14}$	$6.3x10^{12}$	$6.3x10^{12}$	$6.2x10^{12}$	$5.9x10^{12}$	$2.2x10^{10}$
Structural material						
First wall	$6.4x10^{14}$	$5.5x10^{14}$	$3.8x10^{14}$	$3.3x10^{14}$	$2.2x10^{14}$	$6.8x10^{9}$
Breeding zone	$1.6x10^{14}$	$1.3x10^{14}$	$7.7x10^{13}$	$6.5x10^{13}$	$4.1x10^{13}$	$2.2x10^{9}$
Shield	$1.2x10^{13}$	$9.0x10^{12}$	$3.3x10^{12}$	$2.2x10^{12}$	$1.3x10^{12}$	$3.5x10^{8}$

between $2x10^{14}$ and $6x10^{14}$ Bq/kg in the first year after shutdown. After 1 year the activitity in steel decays rapidly. In the shield region the specific activity in steel is two orders of magnitude less than in the first wall. The large amount of Beryllium ($\approx$ 300 tons) starts out at a high level, but after 1 hour of decay the specific activity drops by almost two orders of magnitude remaining stable thereafter for a period of several years. Deliberate tritium removal could further reduce the activation level by 2 - 3 orders of magnitude. Activation products in the primary helium coolant as well as in the purge flow are introduced by corrosion and sputtering. They have to be permanently removed, in order to avoid accumulation somewhere in the circuit components. Therefore, the contents are considered to be small.

9.2 Energy Sources for Mobilization

Potential energy sources in upset or accidental conditions are seen in (a) plasma disruptions, (b) continued plasma operation after cooling disturbances, (c) decay heat, (d) work potential of pressurized coolants, and (e) exothermic chemical reactions.

(a) Plasma disruptions can cause local evaporation of first wall material or mobilization of adhesive dust. This is a problem of first wall protection and dust processing that is common to all fusion reactors and not specific to a particular blanket

system. The energy source is essentially the energy stored in the plasma, typically $\simeq$ 1 GJ. (b) Continued plasma operation after a sudden cooling disturbance will bring any first wall to melt within tens of seconds. The energy source is simply the time integral of fusion power from the cooling disturbance to complete shutdown. This time integral is inherently small (by plasma poisoning) or otherwise a matter of plasma control and of hypothetical scenario conventions, and again not peculiar to a specific blanket concept. (c) The decay heat is the governing feature in managing cooling disturbances like LOCA, LOFA (see section 9.3) and, in particular, loss of site power or loss of heat sink. The decay heat in the entire blanket amounts to 44.3 MW after shutdown and declines after 1 h, 1 d, 1 month, and 1 yr to 21.4, 2.3, 1.8, 0.87 MW, respectively. (d) The blanket cooling system for the outboard/inboard contains $\approx$ 14000/6000 kg of helium at 8 MPa and an average temperature of $\simeq$ 350 °C. The respective work potential relative to ambient conditions is $\approx$ 22/10 GJ. Adiabatic expansion of the helium from five outboard cooling circuits ($\approx$ 7100 kg), which are connected within a subsystem (see Section 3.1), would pressurize the vacuum vessel in the event of an in-vessel pipe rupture to $\approx$ 1.1 MPa absolute. This is far above the expected design pressure ($\simeq$ 0.2 MPa) and, hence, would require a large expansion volume. (e) The largest chemical energy potential results from the vast amount of beryllium multiplier ($\approx$ 300 tonnes). The exothermic reaction per tonne of Be with water or oxygen generates 40 GJ or 67.4 GJ, respectively [81]. However, the vulnerability of the multiplier is low (see 9.3).

9.3 Fault Tolerance

The following analyses of electromagnetic forces, temperature transients, and chemical reactions have been performed in order to show, whether the blanket system is tolerant against conceivable transients and accidental conditions.

Electromagnetic forces and induced stresses caused by disruptions are described in Section 8. Based on the assumptions made the effects are not considered as a critical safety issue.

Temperature transients have been studied for a loss-of-coolant (LOCA) and for a loss-of-flow (LOFA) scenario [82]. A LOCA means at most an instantaneous loss of helium at $t = 0$ in one of the two primary cooling subsystems serving the outboard blanket, while the other subsystem remains intact. Plasma shutdown is assumed to occur at $t = 1$ s with a linear decrease of the surface heat flux to zero in 20 s. A 3-D model representing two adjacent first wall cooling channels (one being operating and the other one failed) and part of the breeder/multiplier region

has been adopted in the FE analyses with FIDAP. Transient temperatures in the first wall exceed the steady state values ($\leq$ 520 °C) for a few seconds by up to 90 °C before they decline and stabilize at a low level. For the LOFA case a linear decrease in mass flow rate from nominal to 1 % of the nominal value (representing the natural circulation flow rate) within 4 s of both cooling subsystems has been postulated. Transient temperatures in the first wall exceed the steady state values for a few seconds by only 65 °C and then decline to below steady state values. The short-term temperature transients from LOCA and LOFA do not endanger the integrity of the structure. Medium-term transients (up to several hours) considering an appropriate decay heat history need to be analyzed. For long-term transients the natural circulation is sufficient to keep the blanket temperatures below acceptable levels provided the helium pressure is maintained at the nominal value and the center of the steam generators lays at least 5 m higher than the blanket center. Credit can also be taken of the purge gas system which is capable of removing a thermal power of approximately 2 MW.

Significant chemical reactions of beryllium multiplier with oxidizing media are only conceivable in case of a major segment box failure (e.g., as a consequence of overpressurization or severe disruptions) accompanied by an ingress of air into the vacuum vessel and/or a major in-vessel water/steam leak (e.g., from the divertor or vacuum vessel cooling system unless they are also cooled by helium). Such scenarios are extremely unlikely and have not been assessed so far. Because of the large energy potential involved (see 9.2) and the subsequent tritium volatility (see 9.4) they need to be analyzed in terms of liberated beryllium masses, dispersion, segregation in the torus, reaction kinetics, and heat balance including decay heat.

9.4 Tritium and Activation Products Release

Radioactive effluents to the environment arise during normal operation and in the course of accidents. In normal operation they will be governed by tritium releases via the steam circuit for which a limit of 1 TBq/d serves as a guideline [78]. The 22 Ci/d (0.81TBq/d) of tritium losses from the primary coolant to the water steam system (see 9.1) are below this limit.

The release rates in accidental situations are hard to quantify at this stage of analyses. As a first approach one may take the radioactive inventories contained in the largest amount of fluid within the blanket system (primary helium coolant and purge gas) which could be liberated by a single failure (like a guillotine break) into either the vacuum vessel or other compartments of the containment.

Table 9-3 Accidental Tritium and Activation Products Release into Vacuum Vessel and Containment in Case of LOCA (after 20 000 hours of full power operation)

	Total Inventory after shut-down	Fraction escaping into		Mobili-zation factor	Single Failure Release into	
		Vacuum vessel	Contain-ment		Vacuum vessel	Contain-ment
Tritium	(g)				(g)	(g)
Breeder material (Li_4SiO_4)	10	0.015	0	1	0.15	0
Neutron multiplier (beryllium)	1278	0.015	0	1	19.2	0
Primary coolant (helium)	0.3	0.24	0.24	1	0.07	0.07
Purge gas (helium)	0.08	1	1	1	0.08	0.08
First wall structural material (MANET)	5.5	1	0	10^{-2}	0.055	0
Activation products	(Bq)				(Bq)	(Bq)
Breeder material (Li_4SiO_4 w/o H-3)	4.8×10^{18}	0.015	0	10^{-6}	7.2×10^{10}	0
Neutron multiplier (beryllium)	4.8×10^{19}	0.015	0	10^{-5}	7.2×10^{12}	0
Primary coolant (helium)	n.a.	0.24	0.24	1	n.a.	n.a.
Purge gas (helium)	n.a.	1	1	1	n.a.	n.a.
First wall structural material (MANET)	4.8×10^{19}	1	0	10^{-5}	4.8×10^{14}	0

n.a. = not assessed

These escaped inventories will then have to be multiplied by a mobilization factor to obtain the potential gaseous or suspended release into the vacuum vessel or containment. Table 9-3 summarizes the escape fractions, mobilization factors, and the resulting single failure releases into the vacuum vessel or containment which have been estimated for this blanket design.

According to an assessment of the effective dose equivalent (EDE) to the most exposed individual (at a distance of 1 km from the point of release) [83] the release of 19.2 g of tritium from the neutron multiplier into the environment (which is the largest single failure release into the vacuum vessel quoted in Table 9-3 without taking credit of any retention offered by the confinement system) would cause an EDE of 35 mSv. This is below the 100 mSv limit recommended in [84] as a safety goal for ITER. For the reactivity release of 4.8×10^{14} Bq from first wall structural material (Table 9-3) into the vacuum vessel a confinement retention factor on the order of < 0.1 would be needed to comply with the dose limit of 100 mSv. It should be noted that the assumptions made in [83] with respect to the release duration (1 h) are very conservative and that, on the other hand, large uncertainties exist in quantifying the mobilization factors.

9.5 Waste Generation and Management

Only the decommissioning waste (no operational waste) is considered here. The masses, volumes, radioactivities, and decay heat are summarized in Table 9-4. The total amount of radioactivity in the blanket structure (MANET) sums up to

Blanket region	Total Mass (10^3kg)	Total Volume (m^3)	Total radioactivity in Bq after decay times			Decay heat after 1 yr (W/m^3)
			1 yr	100 yrs	10^5 yrs	
Breeder material (Li_4SiO_4)	75	31	5.4×10^{14}	1.6×10^{13}	1.3×10^{10}	0.5
Neutron multiplier (beryllium)	314	170	7.7×10^{15}	4.0×10^{12}	9.9×10^{11}	3
Structual material (total)	2248	292	3.5×10^{19}	2.1×10^{15}	2.9×10^{13}	3000
First wall (MANET)	113	15	1.6×10^{19}	5.3×10^{14}	5.9×10^{12}	18000
Breeding zone (MANET)	597	78	1.5×10^{19}	9.2×10^{14}	1.3×10^{13}	5300
Manifold and shield (MANET)	1538	200	3.7×10^{18}	6.7×10^{14}	1.0×10^{13}	960

1.4×10^8 TBq at shutdown for all inboard and outboard segments (Table 9-1). The contribution of each radionuclide has been calculated in [79] for different cooling times. The dominating nuclides in the activation parameters vary with time and activation parameter. For example, Fe-55 and Mn-54 dominate the specific activity at a cooling time of 1 year, and Nb-91, Ni-63, Nb-93 after 100 years. The contact γ-dose rate per kg of MANET in the first wall ranges up to 1.3×10^5 Sv/h, declining slowly. The IAEA low level waste (LLW) limit of 2×10^{-3} Sv/h is reached after about 10^5 years, and the hands-on limit of 2.5×10^{-5} Sv/h is met not sooner than 5×10^5 years. The total amount of radioactivity in the breeder (Li_4SiO_4) is 4.8×10^6 TBq at shutdown but declines by four orders of magnitude within the first year (Tab. 9-4).

10. Reliability and availability

The reliability of the blanket segments and the associated cooling circuits determine the availability of the entire plant. A damage of one blanket segment causes a plant shut down and results normally in an exchange of the relevant segment. A failure in the cooling system is tolerable because of the redundancy in the layout of the circuits. The reliability has been evaluated by fault tree analysis. The TOP event is defined as the unavailability of the entire system when it ought to be available. The basic events for the blanket segments are disturbances in the coolability mainly caused by leakages of the coolant and for the cooling system the failure of circuit components.

10.1 Blanket Segments

Tab. 10.1: Failure Modes and Failure Rates for the He-Cooled Solid Breeder Blanket

Failure modes	Failure rate [1/h]	MTTR [h]	Ref.
Pipe failure (ex-vessel)	$3.0 \cdot 10^{-9}$	200	[85]
SG failure 180 MV	$3.0 \cdot 10^{-5}$	1200	[85]
Valve failure	$3.0 \cdot 10^{-6}$	200	[85]
Blower failure	$1.0 \cdot 10^{-4}$	200	[85]
Vessel failure	$1.0 \cdot 10^{-8}$	200	[85]
EB weld [1/m]	$1.0 \cdot 10^{-9}$	based on	[86]
Diffusion weld [1/m]	$1.0 \cdot 10^{-9}$		[86]
Lingitudinal weld [1/m]	$1.0 \cdot 10^{-8}$		[86]
Butt weld [1/m]	$5.0 \cdot 10^{-9}$		[86]
Pipe bend (assumed $\frac{1}{2}$ 180°)	$5.0 \cdot 10^{-9}$		[86]
Straight pipe [1/m]	$7.0 \cdot 10^{-11}$		[86]

Determining factors for the blanket availability are the conditions of the main weld types which are 1) the longitudinal welds fixing the horizontal cooling plates to the FW, 2) the EB-double-welds connecting the blanket sections and 3) the diffusion welds between the two FW plates forming the FW cooling channels. Based on different basic assumptions concerning these welds the analysis is classified into three different cases.

Case 3 is the most conservative case and considered as the lower bond for the availability. The following assumptions have been made: The specific failure rate of $1 \cdot 10^{-9}$/mh for the horizontal longitudinal welds is set by the factor 10 lower than given in Tab. 10.1. The factor of ten accounts for the fact that a weld failure by itself normally is not critical for the structural integrity, but it could be the initiation of larger failure and evolve into a damage which may endanger the integrity of the FW. The result is a leak of the He to the vacuum.

In [86] it is suggested that an EB-weld has a failure rate one order of magnitude lower than a conventional nuclear weld. Furthermore there are two independent EB-welds connecting FW sections with a monitoring gap between the two welds. Nevertheless a failure rate of $1 \cdot 10^{-8}$ /mh (the value for a single conventional weld) has been used for the EB-double-weld to account for the high thermal and mechanical loading of the FW. A special experimental program for verifying the data of this weld has been initiated in collaboration with an industrial partner. The work is accompanied with theoretical investigations by KfK, first results are available [87].

The blanket structure is designed to withstand the full He pressure (80 bar) [42], therefore, small leakages are tolerable. This is taken into account by setting the failure probability for a damage in the area between the horizontal cooling plates and the He manifolds by a factor of ten lower than for a small leak.

The probability of a failure in the double weld system closing the flow channels in the outer region of the He manifold is also very low and therefore negligible; a damage occurs only if two independent welds fail at the same time.

A leak of a diffusion weld is also tolerable. Therefore, a failure rate of $1 \cdot 10^{-9}$ /mh for the diffusion weld is a conservative assumption as the probability for a weld failure in combination with a damage of the FW structure is relatively low. The inclusion of all the diffusion welds in the analysis is an additional very conservative assumption. For justifying the diffusion weld data a development program with an industrial partner has been initiated. An alternative assumption is to consider

only those welds which are near the EB-double-welds. This has been done in Case 2 while all other assumptions are the same as in Case 3.

The assumption for structure damages in connection with the EB-double-welds is very conservative. A plant shut down is only possible if both welds fail at the same time. This is very unlikely, therefore the use of the specific failure rate according to Tab. 10.1 with $1 \cdot 10^{-9}$ /mh is more realistic, but still quite conservative. This case is defined as Case 1. The main failure rates used in the analysis as well as the mean times to repair (MTTR) for the ex-vessel cooling system are listed in Tab. 10.1.

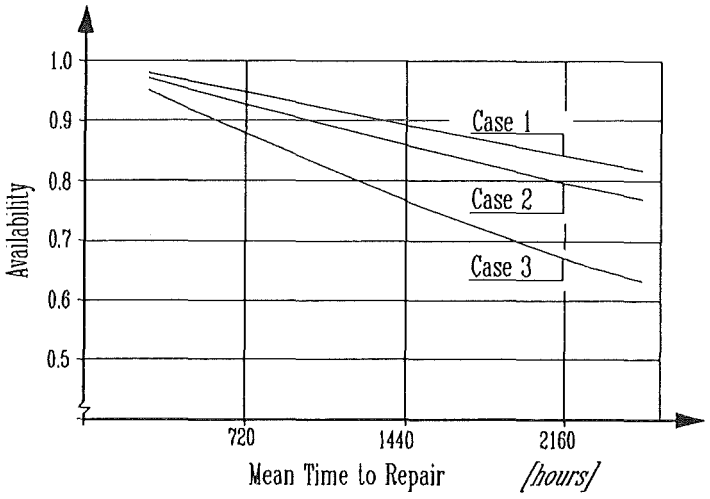

Fig. 10.1: Availability of the solid helium breeder blanket depending on the MTTR

The results of the analysis for the blanket availability are given in Fig. 10.1. The mean repair time for blanket segments has been varied between 720 and 2160 hours. The parameter is selected in order to account for the large uncertainties existing in the assumptions. The blanket availability for the Case 3 is the lowest. The contribution to the complement, the unavailability, is about 20% from the horizontal longitudinal welds fixing the cooling plates on the FW cooling system. 14% are caused by the EB-double-welds connecting the blanket sections. 9% are the contribution from the blanket inlet and outlet tubes and welds to the He manifold. 10% are initiated by the inlet and outlet flow leading system between the horizontal cooling plates and FW and the He manifolds inside the blanket segments. This contribution is mainly influenced by the 90° bends, the butt welds for the tubes and the welds fixing the headers on the FW system. The largest part of the remaining 45% comes from the diffusion welds inside the first wall cooling system.

Case 2 shows an increase of the blanket availability. This improvement is the result of the consideration of the diffusion welds only in neighbourhood of the EB-double-welds.

A further increase of the blanket availability is achieved in Case 1, which is considered to be the most realistic case. In Case 1 the dominating influence is transferred from the diffusion welds (Case 3) to the longitudinal welds fixing the horizontal cooling plates. The contributions of the diffusion welds to the unavailabili-

ty is reduced from 45 to 6%, and for the EB-double-welds from 14 to 3%. The influence of the longitudinal welds is increased from 20 to 48%, of the inlet and outlet tube system from 9 to 22% and of the connections between the He manifold and the horizontal cooling plates from 10 to 21%. The increase of the values means that the absolute contribution is constant while the overall result has been adequately reduced.

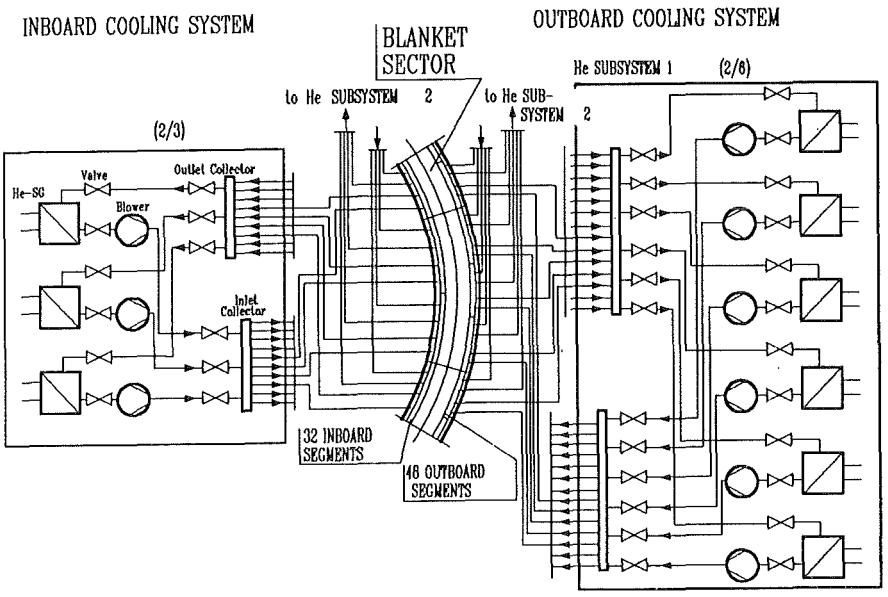

Fig. 10.2: Scheme of the cooling system of the He cooled solid breeder blanket concept.

At the present state of development and depending on the R&D results no principal difficulties in improving the availability over the results for Case 1 are expected, because of the conservative tendency which remains in Case 1.

10.2 Cooling System

The cooling system consists of two independent systems as shown in Fig. 10.2 (see also Section 3). Each system is subdivided into two independent subsystems. The figure contains only one of the two subsystem. The circuits of the subsystems for the inboard blanket are arranged in a 2 out of 3 redundancy and the circuits of the subsystems for the outboard blanket in a 2 out of 6 redundancy (two out of six means, only if at least two out of the six circuits in a subsystem fail, the entire system will fail). Altogether there are 18 cooling circuits with a thermal power of 180 MW each. That means every input and output collector (of the total number of 8) provides about 48 or 32 input and output connections to the outboard and inboard blanket segments, respectively.

The availability of the blanket cooling system is calculated $> 96\%$ [88]. This value is considered adequate at the present stage of the project, all the more since the underlying failure data are associated with high uncertainties. However, a certain potential for improving the availability is emerging already now. This could be an

increase in the degree of redundancy by appropriately combining the inlet and also the outlet collectors of the inboard and of the outboard cooling systems, respectively. This connection would be normally closed during operation and open when the need arises. In this way, the two out of three redundancy of the inboard systems would become a three out of six redundancy and the two out of six redundancy of the outboard systems would become a three out of twelve redundancy. Thus, the total availability could be increased to approximately $> 99\%$.

10.3 Conclusions

The overall availability of the totality of all blanket segments according to Case 3 is based on very conservative assumptions and therefore considered as a lower bound. The result is composed about 50 to 60% by the outboard blanket, 25 to 30% by the inboard blanket, depending on the MTTR of 720 to 2160 hours. The Case 3 is based on the assumption that the EB-double-weld at the FW is classified with the same specific failure rate as a conventional single weld, and in addition, that a failure in the diffusion welds in the FW panel is set equal with a damage of the structure so that a blanket exchange is required. The consideration of the diffusion welds only in the region of the EB-double-welds according to Case 2 remarkably increases the overall availability. A reduction of the assumed failure rate of the EB-double-welds by a factor of 10, would result in a further increase of the overall availability as shown in Case 1. This Case is considered as the most realistic one. However, due to the importance of the EB-double welds, an experimental program in collaboration with an industrial partner and theoretical work at KfK [87] have been initiated.

This parameter variation shows that a certain margin for improvements is available dependent on the results of R&D, of design options for the blanket, and changes in the degree of redundancy for the external cooling systems.

Difficulties and uncertainties in the reliability analysis arise mainly from the lack of completeness in the design and from the novel feature of components and systems without adequate operating experience. The preliminary results from the experimental verification so far support the assumptions which have been made. But work must continue and further R&D is necessary.

11. Remaining Critical Issues. Required R&D Program

The R&D work for the European martensitic steels, including MANET, which has been chosen as a structural material for all four blanket concepts, is part of a so

far separate program within the EFTP (European Fusion Technology Program) and will not be discussed here.

The design and R&D work for the BOT Solid Breeder Blanket has brought forward an attractive concept, which appears to be feasible. There remain, however, still critical issues which have a strong impact on the concept feasibility and its performance. These are shortly discussed in the following sections. The last section 11.5 describes the R&D work for the test modules to be irradiated in ITER.

11.1 Behaviour of Beryllium Under Irradiation

The data on swelling, embrittlement and tritium release from modern beryllium are not yet sufficient to cover the peak conditions in the DEMO blankets. The computer code ANFIBE correlates well the data on swelling and tritium release available from the literature and is able to extrapolate these data to the DEMO conditions. However, more data is required from high temperature irradiations to high fluences in fast reactors. A joint European irradiation experiment in the fast reactor Phenix will start before the end of 1994 to achieve a peak fluence of 4600 appm helium, i.e. about 1/3 of the peak value in the BOT blanket. A further irradiation in Phenix up to the peak fluence is thus required.

The irradiation experiment in the BR2 reactor in Mol has been terminated in March 1994. The results of PIE examinations will be available at the beginning of 1995. These data will be probably sufficient to assess the beryllium embrittlement issue for the two European Solid Breeder Blankets.

11.2 Behaviour of the Li_4SiO_4 Pebbles Under Irradiation

The irradiations performed so far have been encouraging. The tritium release, mechanical stability and compatibility results were satisfactory. However, the bulk of these data have been obtained for lithium burn-ups of up to 3% and damage of up to 2-3 dpa, i.e. for conditions considerably lower than the peak values for the DEMO blanket.Capsule irradiations in the fast reactor FFTF have shown the good mechanical stability of the pebbles up to a burn-up of 6%. However, they have not given information on tritium release behaviour. The European EXOTIC-7 irradiation experiment will be terminated at the beginning of 1995. Here, burn ups of up to 10-15% and damages of 6-9 dpa will be obtained. However, the peak dpa rates of the DEMO blankets are achievable in a reasonable time only in a fast reactor. A joint international irradiation experiment is foreseen for this purpose in the fast reactor Phenix. A further experiment (EXOTIC-8) is

planned to irradiate greater quantities of breeder material to allow out-of-pile tests (thermal cycling, heat transfer) on irradiated material.

11.3 Tritium Control

The condition that only about 20 curie/d is permeating from the main helium coolant circuit through the steam generators requires permeation barriers on the cladding of the breeder material and / or on the steam generator surfaces, and / or a tritium oxidation or a dilution with hydrogen in the main helium coolant system. The analysis of these various possibilites and possibly experimental work should be part of the future European R&D work.

11.4 Design Improvements and Validation

All the four European blanket concepts use a strong blanket box where diffusion welding plays a major role. The fabrication of the first and side wall of the box (diffusion welding, bending) should be further investigated together with external partners and industry. For the BOT solid breeder concept, also the fabricability of the welds of the coolant plates and of the short manifolds to the box walls should be investigated in collaboration with an industrial partner. In general the design should be improved in view of increasing further the blanket availability.

The analysis of the mechanical effects caused by plasma disruptions should be extended to include the effects of the neutron irradiation on the structural material.

The safety analysis should be continued to include other important accidents as the loss of coolant to the plasma region and others.

Out-of-pile tests of blanket submodules should be performed in the HEBLO loop in Karlsruhe and subsequently, in a joint European experiment, in the bigger facility HE-FUS3 in Brasimone. These experiments, which involve mainly the determination of flow, temperature and pressure distributions in the blanket, and thermal cycling tests, will be of fundamental importance also for the test modules to be irradiated in ITER.

11.5 Blanket Test Modules to Be Irradiated in ITER

One of the main objectives of ITER is to test DEMO-relevant blankets. This requires a certain amount of design work for the foreseen test objects or modules

and their ancillary equipment. This work, which has to be performed in close collaboration with the ITER team, should help to identify the minimum requirements posed by these tests on the ITER plasma operation (length of burn shots, duty cycle, continuous operation time, integral burn time) and the space and location required by the ancillary equipment.

12. Conclusions

The European Demo BOT (Breeder Out of Tube) Solid Breeder Blanket is based on the use of 0.3 - 0.6 mm Li_4SiO_4 and beryllium pebbles placed between radial toroidal cooling plates. The cooling is provided by helium at 8 MPa. Detailed neutronics, thermohydraulics and stress calculations have been performed

Table 1 shows the main results of these calculations. The peak temperatures and the calculated stresses in the structural material are well within acceptable limits. The design meets all the requirements specified for the blanket selection process. The use of cooling plates in the blanket, rather than cooling coils, has simplified the design and improved the availability.

The use of two separate independent helium cooling systems and of a strong blanket box capable to sustain the full pressure of the helium coolant offer considerable advantages. An instantaneous total loss of the coolant from one system or a fast loss of flow of both systems cause only temperature increases of 60 - 90 °C for a few seconds in localized parts of the blanket.

The Li_4SiO_4 pebbles can be fabricated by an industrial firm to the required specifications at the rate of 5 kg in 8 hours. A plant production of 30 - 40 tonnes per year is readily feasible. The reference Li_4SiO_4 + 2.2 % SiO_2 pebbles behave well under irradiation. The irradiation experiments performed so far indicate that the mechanical integrity of and the tritium release from the pebbles are unaffected by lithium burn-ups up to more than 80 % and 40 % of the DEMO peak values respectively. Running irradiation experiments (EXOTIC-7) will allow in 1995 to assess the effects of lithium burn-ups considerably higher than the peak DEMO values.

The beryllium pebbles are readily available from the market. The developed computer code ANFIBE can predict the swelling and tritium retention data from the beryllium experimental results available in the open literature. Its predictions for the BOT DEMO blanket indicate that peak beryllium swelling would be limited to 8.7 %, thus it would not impede the flow of the tritium purge gas. Although the total tritium inventory in beryllium would be rather high at the end of the blan-

ket life (1.3 kg), only about 40 g would be released quickly by an overheating accident and the subsequent release would be slow.

Li_4SiO_4 and beryllium are low activation materials. In both cases the pebbles can be produced by melting and spraying. Thus the reprocessing is relatively easy and efficient.

The tritium extraction from helium has been proved during the operation of the helium cooled fission reactors (HTR). Even the extraction of large quantities of tritium directly injected in the main helium coolant system from the plasma does not pose feasibility problems. The calculated tritium losses through the steam generators of about 20 Ci/d would probably be acceptable. However in case of large quantities of tritium injected into the main helium coolant system and/or temperature transients, which can exert a detrimental effect on the oxide barrier of the steam generators surface, would imply the necessity of reducing the tritium losses to the steam/water system. Various possibilities to do so will be investigated within the European program.

The use of inert materials as helium and ceramic Li_4SiO_4, the low activation and the low lithium burn-up required by Li_4SiO_4 in comparison with other ternary lithiated ceramics, the use of small pebbles with their advantages in reducing the stresses and filling the available space in the optimum way, the use of two independent helium cooling systems and of a strong blanket box with their safety advantages make the BOT solid breeder blanket an attractive concept for the DEMO reactor.

The remaining issues:

- behavior of the beryllium pebbles under irradiation at high temperatures up to the maximum neutronic fluences foreseen in the DEMO, and
- effect of the lithium burn-up and of the neutron damage (dpa) on the Li_4SiO_4 pebbles up to the maximum DEMO values

are being and will be investigated in irradiation experiments in the fast reactor Phenix and in HFR Petten.

Further work is also required to reduce the tritium losses through the steam generators.

Table 1 Main characteristics of BOT DEMO Solid Breeder Blanket

Breeding and multiplier material	Separated beds of Li_4SiO_4 and beryllium pebbles
Li^6 enrichment	25 at%
Total blanket power	2500 MW (+ 300 MW in divertors)
Coolant helium pressure outboard inboard	8 MPa 8 MPa
Coolant helium pressure drop (F.W., blanket, feeding tubes) outboard inboard	0.30 MPa 0.30 MPa
Coolant helium temperature: inlet outlet	250 °C 450 °C
Plant thermal efficiency	34.6 %
Max. steel temperature	520 °C
Max. temp. in beryllium	640 °C (BOL) 500 °C (EOL)
Max. temp. in breeder material Min. temp. in breeder material	900 °C 350 °C
Real tridimensional tritium breeding ratio (without ports) Accounting for 10 outboard ports	1.13 (BOL) 1.11 (EOL) 1.07 (BOL) 1.05 (EOL)
Peak lithium burn up	7.25 at%
Peak fluence in beryllium	16300 appm He
Tritium purge system pressure	0.1 MPa
Tritium inventory in breeder mat.	10 g
Tritium inventory in Beryllium (EOL)	1280 g
Tritium losses to steam/water system	22 curie/d

References

1. E. Proust, L. Anzidei et al., Status of the Design and Feasibility Assessment of the European Helium Cooled Ceramic Breeder inside Tube Test Blanket, Fus. Technol. 19 (1991) 944.
2. L. Petrizzi, L. Giancarli, V. Rado, C. Diop, Further Neutronic Analyses of the European Ceramic BIT Blanket for DEMO, Proc. 17th SOFT Conf., p. 449, Rome 14 - 18. Sept. 1992.
3. M. Dalle Donne et al., DEMO-relevant Test blankets for NET/ITER. BOT Helium Cooled Solid Breeder Blanket, Kernforschungszentrum Karlsruhe, Report KfK 4928 and 4929, Oct. 1991.
4. M. Dalle Donne et al., Conceptual Design of a Helium Cooled Solid Breeder Blanket Based on the Use of a Mixed Bed of Beryllium and Li_4SiO_4 Pebbles, Proc. 17th SOFT, Rome, 14 - 18. Sept. 1992, Vol 2, 1326.
5. M. Dalle Donne, U. Fischer, P. Norajitra, G. Reimann, H. Reiser, European DEMO BOT Solid Breeder Blanket: The Concept Based on the Use of Cooling Plates and Beds of Beryllium and Li_4SiO_4 Pebbles, 18th SOFT, Karlsruhe, 22 - 26 August 1994.
6. E. Proust, L. Anzidei, G. Casini, M. Dalle Donne, L. Giancarli, S. Malang, Breeding Blanket for DEMO, Fusion Engrg. & Des. 22 (1993) 19 - 33.
7. Siemens Report, April 1993
8. Siemens Contract on EB-Welding, 1994
9. S. Malang, E. Bojarski, L. Bühler, H. Deckers, U. Fischer, P. Norajitra, H. Reiser, Dual-coolant Liquid Metal Breeder Blanket, Proc. 17th SOFT, Rome, 14 - 18 Sept. 1992, Vol. 2, 1424.
10. J. F. Briesmeister (Ed.): MCNP - A General Monte Carlo Code for Neutron and Photon Transport, Version 3A, Report LA-7396-M, Rev. 2, Sept. 1986
11. P. Vontobel: A NJOY Generated Neutron Data Library Based on EFF-1 for the Continuous Energy Monte Carlo Code MCNP, PSI-Bericht Nr. 107, September 1991
12. U. Fischer: Die neutronenphysikalische Behandlung eines (d,t)-Fusionsreaktors nach dem Tokamakprinzip (NET), Bericht KfK-4790, Oktober 1990
13. U. Fischer: Optimal Use of Beryllium for Fusion Reactor Blankets, Fusion Technology 13(1988), 143 - 152

14. U. Fischer: Impact of Ports on the Breeding Performance of Liquid Metal and Solid Breeder Blankets in the DEMONET Configuration, Fusion Engineering and Design 18 (1991), 323-329

15. H. Tsige-Tamirat, U. Fischer: Three-dimensional Activation and Afterheat Analysis for the Helium Cooled Solid Breeder Blanket, KfK-Report (to appear)

16. R. A Forrest, J.-Ch. Sublet: FISPACT3 - User Manual, AEA/FUS/227, April 1993

17. J. Kopecky, H. A. J. van der Kamp, H. Gruppelaar, D. Nierop: The European Activation File EAF-3 with Neutron Activation and Transmutation Cross Sections, ECN-C-92-058 , September 1992

18. Brush-Wellman material specification for beryllium pebbles.

19. M. Schirra et al.: Untersuchungen zum Vergütungsverhalten, Umwandlungsverhalten und der mechanischen Eigenschaften am martensitischen Stahl 1.4914 (NET-Charge MANET-1), KfK-4561, Juni 1989

20. H. Tsige-Tamirat: Impact of Sequential Charged Particle Reactions on the Activation Behaviour of Li_4SiO_4, 18th Symposium on Fusion Technology, Karlsruhe, Germany, August 22 - 26, 1994.

21. L. R. Greenwood, R. K. Smither: SPECTER - Neutron Damage Calculations for Material Irradiations, ANL/FPP/TM-197, January 1985

22. D. Hermanutz: Neutron Induced Displacement Damage in ^{9}Be, 18th Symposium on Fusion Technology, Karlsruhe, Germany, August 22 - 26, 1994.

23. P. Norajitra, Internal KfK report, July 1994.

24. P. Norajitra, Internal KfK report, Oct. 1994.

25. M. Dalle Donne and F.W. Bowditch, Experimental Local Heat Transfer and Friction Coefficient for the Flow of Air or Helium in a Tube at High Temperatures, OECD Dragon Project, Report 184, Organization for Economic Cooperation and Development (1963).

26. H.J. Pfriem, Der turbulente Wärmeübergang an Helium und Wasserstoff in beheizten Rohren bei großen axial steigenden Temperaturdifferenzen und das sich daraus ergebende Temperaturprofil, KfK 1860, Kernforschungszentrum Karlsruhe (1973).

27. M. Dalle Donne et al., Heat Transfer and Technological Investigations on Mixed Beds of Beryllium and Li_4SiO_4 Pebbles, Proc. ICFRM 6. Stresa, Italy, Sept. 27, - Oct. 1, 1993.

28. E.U. Schlünder, Particle Heat Transfer, Proc. 17th Int. Heat Transfer Conf. Munich, 1982, Vol. 1, RK 10, 195.

29. M. Küchle, Material Data Base for the NET Test Blanket Design Studies, Test Blanket Advisory Group, KfK, February 1990.

30. W. Kalide, Einführung in die technische Strömungslehre, Carl Hansen Verlag, München, 1971.

31. Hibbit, Karlsson, Sorensen, ABAQUS User's Manual Version 4.9, Providence, R.I., U.S.A.

32. ASME Code III, Edition 1986.

33. E. Zolti et al., Interim Structural Design Criteria for Predesign of the NET Plasma Facing Components, NET/IN/86-14, March 1986.

34. K. Ehrlich, Internal KfK report, May 1986.

35. Siemens-KWU, Conceptual Design of the Cooling Systems for a DEMO Fusion Reactor with Helium Cooled Solid Breeder Blanket and Calculation of the Transient Temperature Behaviour in Accidents, KfK-Contract No. 315/03179710/0102, July 1992.

36. P.G. Chapman, Design Operating Experience, Proc. Gas Cooled Reactor Information Meeting, Oak Ridge, Tenn., CONF-700401, April 27 - 30, 1970.

37. X. Raepsaet et al., Some Considerations on Tritium Control for the European Ceramic BIT DEMO Blanket, Fus. Eng. Design 17 (1991) 367.

38. G.R. Longhurst et al., Research of Beryllium Safety Issues, Workshop on Beryllium for Fusion Applications, Kernforschungszentrum Karlsruhe, Report KFK 5271, Dec. 1993.

39. M. Dalle Donne and S. Dorner, Tritium Control in a Helium Cooled Ceramic Blanket for a Fusion Reactor, Fus. Technol. 9 (1986) 494.

40. K. Forcey, D. Ross, J. Simpson and D. Evans, Hydrogen Transport and Solubility in 314L and 1.4914 Steels for Fusion Reactor Applications, J. Nucl. Mat. 160 (1988) 117.

41. M. Futterer, X. Raepsaet, E. Proust, Tritium Permeation Through Helium-Heated Steam Generators of Ceramic Breeder Blankets for DEMO , ISFNT-3, June 27 - July 1, 1994, Los Angeles.

42. M. Dalle Donne, L. Anzidei, H. Kwast, F. Moons, E. Proust, Status of the EC Solid Breeder Blanket Designs and R&D for DEMO Fusion Reactor, ICFRM-6, Stresa, Italy, Sept. 1993.

43. H. Albrecht, E. Hutter, Tritium Recovery from a Solid Breeder DEMO Blanket, 18. SOFT, Karlsruhe, Germany, Aug. 22-26, 1994

44. M.C. Billone, W. Dienst, T. Flament, P. Lorenzetto, K. Noda and N. Roux, ITER Solid Breeder Blanket Materials Data Base, ANL/FPP/TM-263, November 1993.

45. R.-D. Penzhorn, H.R. Ihle, S. Huber, P. Schuster, Free Evaporation from Lithium Orthosilicate Surfaces, Fusion Technology 1990, p. 832.

46. H.R. Ihle, R.-D. Penzhorn, P. Schuster, Internal KfK report, 1991.

47. R.-D. Penzhorn, H.R. Ihle, P. Schuster, Thermodynamic Study of Gas/Solid Reactors at the Surface of Li_4SiO_4 in View of Blanket Sweep Gas Chemistry, 17th SOFT, Rome, 14-18 Sept. 1992, p. 1389.

48. M. Dalle Donne, A. Goraieb and G. Sordon, Measurements of the Effective Thermal Conductivity of a Bed of Li_4SiO_4 Pebbles of 0.35 - 0.6 mm Diameter and a Mixed Bed of Li_4SiO_4 and Aluminum Pebbles, ICFRM-5, Clearwater, 1991.

49. H. Werle et al., The LISA-2 Experiment: In-situ Tritium Release from Lithium Orthosilicate (Li_4SiO_4), J. Nucl. Mater. 155 - 157 (1988) 538 - 543.

50. W. Krug et al., Inpile Tritium Release from Ceramic Breeder Materials in TRIDEX Experiments 1 - 6, Fusion Eng. Design 17 (1991) 65 - 71.

51. H. Kwast et al., The Behavior of Ceramic Breeder Materials with Respect to Tritium Release and Pellet/Pebble Mechanical Integrity, Report ECN-RX-93-097, November 1993.

52. P. Hofmann, W. Dienst, Chemical Compatibility of Oxide Breeder Materials with Cladding Steels, 17 SOFT, Vol. 2, 1374, Rome, Sept. 1992.

53. P. Hofmann, W. Dienst, Chemical Interactions of Beryllium with Lithium Based Oxides and Stainless Steel, J. Nucl. Mat. 171 (1990) 203.

54. W. Dienst, D. Schild, H. Werle, Tritium Release of Li_4SiO_4, Li_2O and Beryllium and Chemical Compatibility of Beryllium with Li_4SiO_4, Li_2O and Steel (SIBELIUS Irradiation), KfK 5109, Dec. 1992.

55. W. Dienst and H. Zimmermann, Strength Change and Chemical Reactivity of Ceramic Breeder Materials near Operation Conditions, ICFRM-6, Stresa, 1993.

56. L. Dörr, D. Schild, H. Werle, Tritium Release and Gamma Activity of Various Lithium Ceramics Irradiated by Fast and Thermal Neutrons (COMPLIMENT Experiment), KfK 5355, June 1994.

57. P. Weimar, H. Steiner, H. Zimmermann, L. Dörr, Results of Post Irradiation Examination of Breeder Pellet/Pebbles of the Irradiation Experiments COMPLIMENT and ALICE-3, SOFT-18, Karlsruhe, 1994.

58. H. Wedemeyer, E. Günther, R. Knitter, Proc. Jahrestagung Kerntechnik 1992, p. 445.

59. M. Dalle Donne, P.l Norajitra and A. Weisenburger, Thermal Cycling Tests on Li_4SiO_4 and Beryllium Pebbles, 18th SOFT, Karlsruhe, 1994.

60. H. Gerhardt, K. Schleisiek, KfK, unpublished.

61. G. Butterworth, Activation Characteristics and Waste Management Options for Some Candidate Tritium Breeders, J. Nucl Mater. 184 (1991) 197.

62. S. Dorner, Herstellung, Wiederaufarbeitung und Entsorgung von Lithiumorthosilikat (Li_4SiO_4)-Kügelchen für Fusionsreaktorblankets, unpulished, May 1992.

63. P. Gierszewski et al., Ceramic Pebble Bed Development for Fusion Blankets, ISFNT-3 Conference, Los Angeles, June 27 - July 1, 1994.

64. A. Terlain et al., Compatibility Problems with Beryllium in Ceramic Blankets, 16th SOFT, Vol. 2, 1179, Utrecht, Sept. 1988.

65. V. Levy, Rapport final du Contrat SBB-BS1, CEA Report, Centre d'Etudes de Saclay, N.T. SRMA 92-1955, F.A. 3591-532 (1992).

66. M. Dalle Donne, F. Scaffidi-Argentina et al.: Modeling He-induced Swelling in Beryllium during Fast Irradiation, in Proc. Beryllium Workshop, Karlsruhe 4 - 5 October 1993, Kernforschungszentrum Karlsruhe Report KfK 5271.

67. D.L. Baldwin and M.C. Billone, "Diffusion/Desorption of Tritium from Irradiated Beryllium", ICFRM-6 Stresa, Italy, Sept. 1993.

68. M.C. Billone et al., Fusion Technol. 19 (1991)1707.

69. M. Dalle Donne, F. Scaffidi-Argentina et al.: Computer Simulation of Tritium Retention and Release in Irradiated beryllium, in Proc. Beryllium Workshop, Karlsruhe 4-5 October 1993, Kernforschungszentrum Karlsruhe Report KfK 5271.

70. L.V. Boccaccini, Calculation of Electromagnetic Forces and Stresses Caused by a Major Disruption in the Karlsruhe Solid Breeder Blanket Design for the DEMO Reactor, 17th Symp. Fusion Technology, 2 (1992) 1291-1295.

71. L.V. Boccaccini, P. Norajitra, P. Ruatto, Analysis of Mechanical Effects Caused by Plasma Disruptions in the European BOT Solid Breeder Blanket Design with MANET as Structural Material, 3rd ISFNT, Los Angeles 1994, June 1994.

72. L.V. Boccaccini, P. Ruatto, Mechanical Effects Caused by Plasma Disruptions in the European BOT Solid Breeder Blanket Design, 18th SOFT, Karlsruhe, August 1994.

73. L.V. Boccaccini, Mechanical Assessment of the European BOT Solid Breeder Blanket for the Demo Reference Disruption, KfK report, to be published.

74. R. Albanese, G. Rubinacci, IEE Proceedings, 135 (1988) 457-462.

75. P. Ruatto, Proc. 2nd Int. Workshop on Electromagnetic Forces and Related Effects on Blankets and Other Structures Surrounding the Fusion Plasma Torus, UTNL-R-0302, Tokai, Japan, Sept. 1993, pp.169-177.

76. M. Rieth, B. Dafferner, C. Wassilew, KfK 5243 (1993).

77. L.V. Boccaccini, Proc. 2nd Int. Workshop on Electromagnetic Forces and Related Effects on Blankets and Other Structures Surrounding the Fusion Plasma Torus, UTNL-R-0302, Tokai, Japan, Sept. 1993, pp.189-200.

78. L. Giancarli, W. Kramer, C. Nardi: Safety Related Criteria for the Evaluation of Different Blanket Concepts, Proposal for the DEMO Blanket Selection Exercise, Working Group 6a: Safety, Feb. 25, 1993.

79. Tsige-Tamirat, Activation analysis, private communication, September 1994.

80. H. Albrecht, Internal Note of 17.08.94.

81. I. Barin, Thermophysical Data of Pure Substances, VCH Weinheim, 1989.

82. F. Dammel, KfK internal report in preparation.

83. W. Raskob, Accidental Release of Activation Products MANET and Pb-17 Li, unpublished note, August 1994.

84. International Atomic Energy Agency: ITER Safety, ITER Documentation Series, No. 23, Vienna, 1991.

85. L. C. Cadwallader, S. J. Piet; 1988 Failure Rate Screening Data for Fusion Reliability and Risk Analysis, EGG-FSP-7922, January 1988, Idaho National Engineering Laboratory

86. R. Bünde, S. Fabritssiev, V. Rybin; Reliability of Welds and Brazed Joints in Blankets and its Influence on Availability; Fusion Engineering and Design 16 (1991) 59-72, North-Holland

87. L. Cizelj, H. Riesch-Oppermann; An Analysis of Electron Beam Welds in a Dual Liquid Metal Breeder Blanket, Institut für Materialforschung II, KfK 5360, in preparation

88. H. Schnauder; Reliability Analyses of the Cooling Systems of Two DEMO Breeder Blanket Concepts, KfK/IRS, SOFT´18, Karlsruhe, August 22,-26, 1994